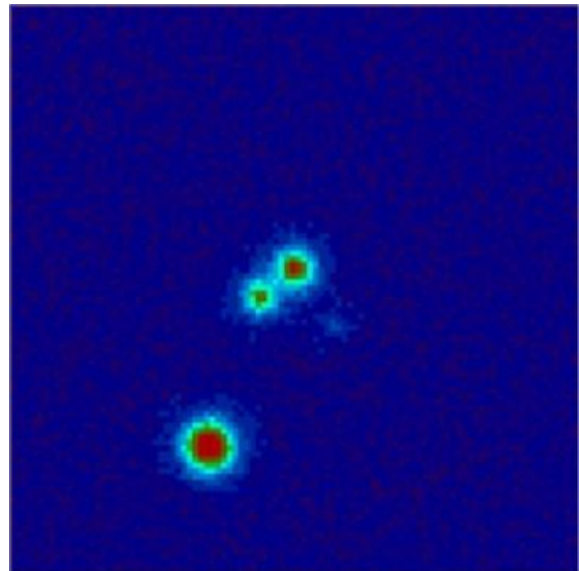
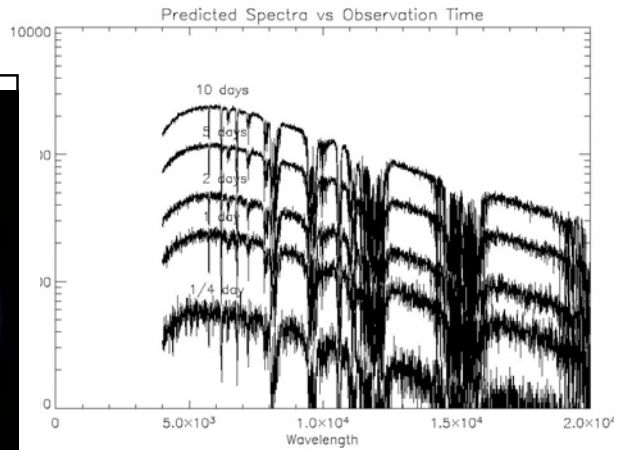


**Final Report to the
NASA Institute for Advanced Concepts
March 31, 2005
Phase I Study
THE NEW WORLDS IMAGER**



**Webster Cash
Principal Investigator
University of Colorado**



ABSTRACT

We report on the first study of the New Worlds mission. It is based on the concept of the “starshade”, a large, opaque screen flying separately at a great distance, but configured to remove the light from the star while allowing planetary light into the telescope. The starshade can be a pinhole camera or an occulter. During the course of the study we directed a great deal of attention to the occulting starshades as they are smaller, lighter, less expensive and allow deeper surveys. We are pleased to report that during the course of this study we found an occulter design that meets the extreme contrast requirements of exo-planet studies. The study goes on to show that our starshades can be built, launched, deployed and held in position as needed. In its simplest embodiment (dubbed New Worlds Observer) we need a single starshade and a single telescope. The simulations of performance are very exciting, showing the ability to detect even comets in other planetary systems. With five spacecraft, the New Worlds Imager is a direct extension of the starshade concept and should be capable of creating true images of planets around other suns. New Worlds Observer may prove to be easier, more sensitive, lower risk and lower cost than the Terrestrial Planet Finder. It is not too late for NASA to consider this alternative.

CONTRIBUTORS

W. Cash	University of Colorado
J. Green	
D. Feldkuhn	
N. Rajan	
E. Schindhelm	
A. Shipley	
J. Kasdin	Princeton University
R. Vanderbei	
W. Simmons	MIT
J. Leitch	Ball Aerospace
E. Wilkinson	
J. Arenberg	Northrop Grumman
R. Polidan	
S. Seager	Carnegie Institution

Contact:

Prof. Webster Cash
Center for Astrophysics and Space Astronomy
University of Colorado
Boulder, CO 80309-0389

cash@casa.colorado.edu

303-492-4056

Table of Contents

I. THE SEARCH FOR NEW WORLDS	5
A. The Path to the Goal	5
1. Detection	5
2. System Mapping	6
3. Planet Studies	6
4. Planet Imaging	6
5. Planetary Assessment	7
B. The Problem	7
C. The NASA Program	7
D. The New Worlds Alternative	8
E. The Phase I Study	9
II. THE NEW WORLDS OBSERVER	11
A. Starshades	11
B. The Pinhole Camera	13
C. The Pinspeck Camera	14
D. Diffraction Control	15
1. Pinhole	15
2. Pinspeck	20
E. Starshade Deployment	24
F. Formation Flying	27
G. Telescope & Spectrograph	29
H. Simulations	30
1. Planet Finding	30
2. Planet Spectroscopy	35
3. Photometry	36
III. THE NEW WORLDS IMAGER	39
A. Concept	39
B. The Interferometer	40
C. Target Acquisition	40
D. Formation Flying	40

E. Simulations	41
IV. PRELIMINARY ROADMAP	44
A. Scaling the Architecture	44
1. Planet Finding	44
2. Photometry	44
3. Astrometry	44
4. Spectroscopy	45
5. Imaging	45
6. Surveys	45
7. Distance	45
8. Sensitivity	45
B. Key Technologies	45
1. Diffraction Controlled Apertures	46
2. Large Structures	46
3. Formation Flying	47
4. Telescope	47
C. The Road Ahead	47
V. BIBLIOGRAPHY	48

*Certain knowledge of a habitable destination
could drive future generations to
cross the awesome gulf of interstellar space.*

I. The Search for New Worlds

We live in a time when all the corners of the Earth have been discovered and mapped in great detail. Few people alive remember first hand the sense of excitement and high adventure that comes from the discovery of new lands. Yet no other endeavor resonates more with the imagination of the young, or carries more promise for the future.

America has led the way in keeping the spirit of discovery alive. NASA probes, rocketed out into our solar system, have revealed alien landscapes and given us new perspective on our own small planet. But extremes of temperature and the absence of breathable atmosphere have, so far, made the expansion of mankind into space a dangerous and economically unrewarding effort.

Since we now know the basic outlines of the Solar System, we naturally desire to extend our knowledge to other planetary systems. Observations will immediately give us fundamental new understanding of the nature of planets and their systems as we break outside of the confines of the single example in which we live.

But more than anything, we all wish to find that elusive place, the blue, watery planet with a shirt-sleeve environment that might eventually become a comfortable home. Certain knowledge of a habitable destination could drive future generations to innovate and find a way to cross the unimaginable distance to that New Earth.

In this study we have taken the first look at a technology that can allow the search and study of New Worlds to proceed in the near future.

A. The Path to the Goal

The finding and subsequent study of planets around other stars will occur in a predictable series of stages:

1. Detection

For a half a century the press regularly reported the “Discovery of the First Planet Outside the Solar System”. Until about ten years ago each proved to be a suspect or marginal result and the very existence of planetary systems remained in question. But the advent of the Doppler studies of stellar lines finally and

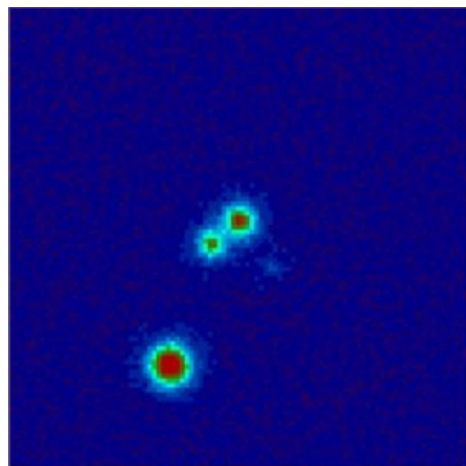


Figure 1: A possible image of a planetary system viewed from Earth.

convincingly proved that planetary systems are a common feature of the stars. With well over one hundred planets and masses inferred by this technique, surprises like the existence of gas giants close to a parent star already abound.

Doppler techniques have trouble detecting low mass planets like the Earth and tells us little aside from the mass and orbit. Direct detection and study are needed.

2. System Mapping

The next step must be the direct mapping of planetary systems by actually detecting the light from the planets separate from the parent star. In a sufficiently high quality image of a planetary system the planets would appear as individual star-like objects. Figure 1 shows a simulation of our solar system as it might appear with the dominant signal from the Sun removed. A series of such images would allow the measurement of orbits. The brightness and broadband colors of the planets would give us information about the basic nature of each planet. System mapping requires a major improvement in our telescope capabilities.

3. Planet Studies

The next level is characterized by the detailed study of individual planets and is a relatively small step beyond System Mapping. If the noise level is low and the signal even modest, then spectroscopy and photometry can be performed on the individual planets. The spectroscopy, as shown in simulation in Figure 2, will allow us to perform chemical analysis of atmospheres and surfaces. The clues to the existence of life elsewhere in the universe might lie in such spectra. Photometry will show variation in color and intensity as surface features rotate in and out of the field of view. Oceans, continents, polar caps and cloud banks may all be detected in such a manner.

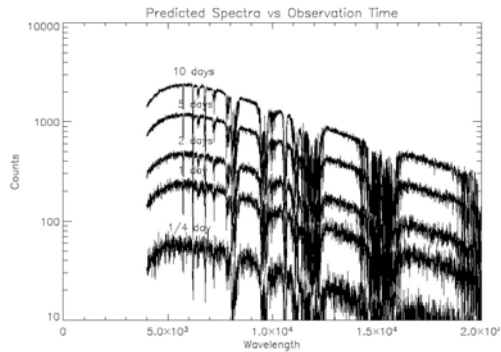


Figure 2: Spectrum of an Earth-like planet.

4. Planet Imaging

A quantum leap in capability is needed to achieve the next level – true planet imaging. In Figure 3 we show the Earth imaged with resolution of about 200km. Such pictures would require telescopes with (synthetic) diameters of over 100km to achieve. But the techniques of interferometry show this is, in principle, possible. We can, literally, map other worlds. Fifty to one hundred percent of a planet’s surface can be mapped, depending on inclination. While we are currently limited to nine planets and their moons, imagine what surprises await us when we start to study the multitude of worlds orbiting nearby stars.



Figure 3: This “simulation” of a terrestrial planet observed with resolution of 200km looks surprisingly like Earth.

5. Planetary Assessment

The final step in exo-planet studies will be the ability to study the planets in same way that Landsat and other Earth-observing systems study the surface of the Earth. Science fiction authors have always assumed we would have to visit distant planets to obtain images like Figure 4, but they can, in principle, be captured from light years away. Such a telescope will of necessity be large, to collect enough light to resolve and analyze small details on distant planets. It is easy to show that, while such studies are possible, they will remain a practical impossibility for the foreseeable future. It takes square kilometers of collecting area to capture the needed signal.



Figure 4: From the movie *Contact*. Dr Arroway gets a brief glimpse of this alien landscape. Such images are possible from Earth, although, at the moment, very expensive.

B. The Problem

There is one over-arching problem that has stymied the direct detection of exo-planets. The planets themselves are sufficiently bright to be observed with modest sized modern telescopes. A one meter diameter, active optic can provide enough resolution to separate them. It is

the overpowering glare of the parent star that hides the planets. If the solar system were to be viewed from 10pc distance, the Earth would appear 10 billion times fainter than the Sun and only one tenth of an arcsecond (a single Hubble resolution element) away. This problem must be solved before any direct observations can even be contemplated.

C. The NASA Program

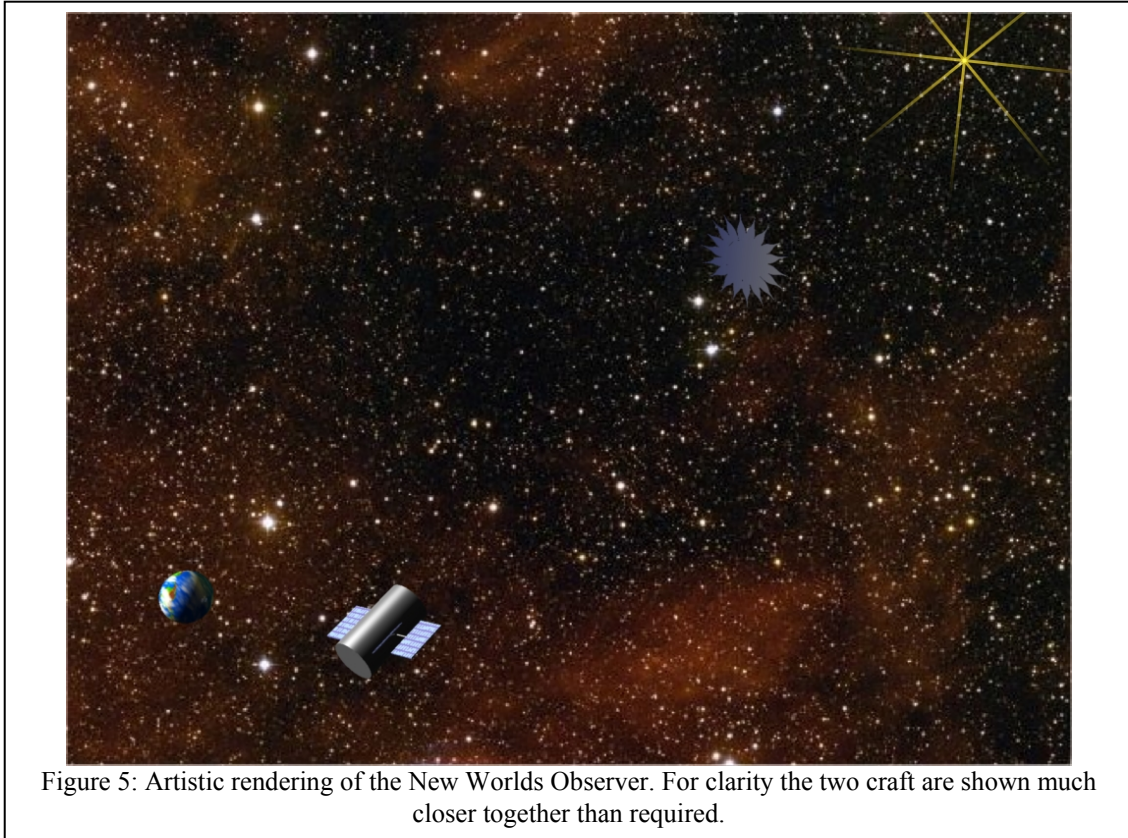
NASA's Office of Space Science, recognizing the importance of the search for distant planets, has given a pre-eminent position to exo-planet science, despite its obvious technical challenges. Several approaches are under development. SIM will use astrometry to detect stars swinging about the center of mass with its planets. Kepler is searching for the transits of planets across the disks of stars. But these are indirect observations, equivalent, in some sense, to the Doppler studies from the ground.

To observe planets directly, NASA is designing the Terrestrial Planet Finder (TPF) and ESA is designing Darwin. TPF is receiving a great deal of development money and figures prominently in NASA's plans. Yet TPF has problems – major problems caused by the contrast ratios between big bright stars and faint, tiny planets a fraction of an arcsecond away. Making a telescope that allows a terrestrial planet to emerge from the glare of its parent star is the challenge of TPF. It in many ways has to be the “perfect telescope”.

To remove scatter from the optics, the mirror must be built to incredibly tight tolerances. For example, the surface must be figured to better than $\lambda/5000$. The coating must reflect with uniformity better than 99.999%. And it still must deal with diffraction.

The cost of TPF is high, somewhere between \$2 Billion and \$5 Billion dollars. The risk is high as well, given that the quality must reach levels previously undreamed of, and then be maintained through launch and the mission. Clearly lower cost, lower risk alternatives should be welcome.

In November 2004, shortly after the Phase I study started, NASA called for white papers on future missions and future technologies. We submitted a white paper on the



use of starshades for planet searching. We have reason to believe that, as a result of the white paper, the New Worlds concept will appear in the NASA roadmap. W. Cash was invited (and went) to give a talk on the New Worlds concept at a future missions session of the American Astronomical Society in San Diego in January 2005.

D. The New Worlds Alternative

In this Phase I we studied a new approach to direct observation of planets around other stars. Based on sound optical and aeronautic practice, the ensuing architecture is revolutionary, yet, if implemented, the scientific return would be huge. Even more so, the mission would be truly exploratory, identifying and mapping unknown worlds. Our concept is to use what we call a “starshade”. It separates the planet light from the starlight before it ever enters a telescope. Thus the horrific problem of scatter is sidestepped.

Such a system can be directly used to map a planetary system, finding planets as small as our Moon, perform sensitive follow-up spectroscopy to study the nature of the planet and search for bio-markers.

The starshades enable an extendable architecture. With two craft (a shade and collector as in Figure 5) we have New Worlds Observer, capable of mapping planetary systems and following up with spectroscopy and photometry. With five craft (see Figure 6) we can create the New World Imager, designed to take high quality pictures (100km resolution) of exo-planets. Ultimately resolution as fine as 1km might be possible, although the size requirement on such a system is daunting.

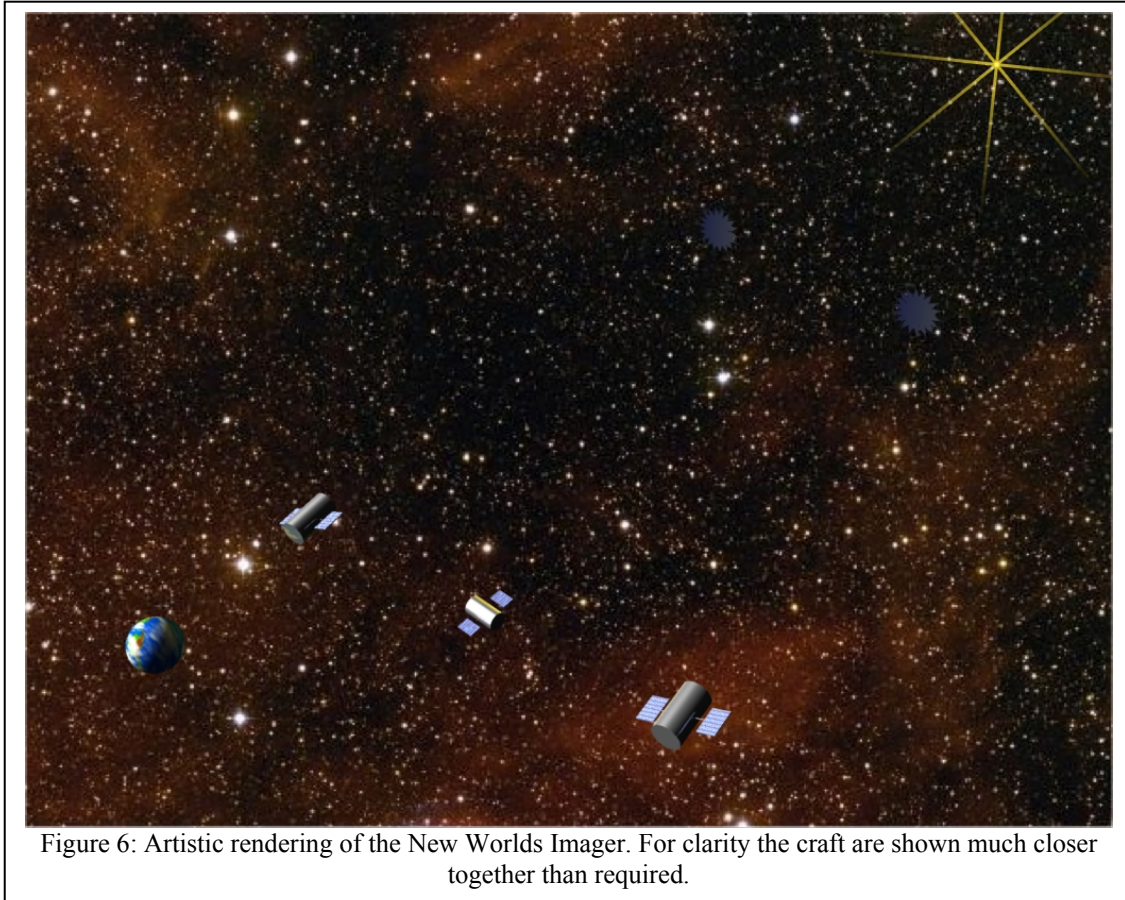


Figure 6: Artistic rendering of the New Worlds Imager. For clarity the craft are shown much closer together than required.

E. The Phase I Study

In the Phase I study we had initially expected to emphasize the study of several key technologies including deployment of the large starshades, formation flying and the requirements for image formation in the interferometer. The study took a rather interesting turn. While we did study these key technologies, we found early on that starshades in excess of 150m diameter were difficult to launch and deploy, leading to higher costs and greater waiting time until launch.

Because of the great advantage we returned to the possibility of using occulters, starshades that directly shadow the star, rather than forming a pinhole image. Such a “pinspeck” camera would be much smaller and less massive, enable simultaneous imaging of the entire planetary system minus the central star, and allow for smaller telescopes.

The financial incentive was huge, but occulters were known to have diffraction problems (Copi and Starkman, 2000). We thus spent a large fraction of our effort in Phase I studying the diffraction patterns of pinspeck cameras. In the end we found that the approach recently explained by VanderBei et al (2003) in making diffraction controlled apertures for TPF could be adapted to occulting craft.

As a result of the success of the diffraction control development, we now have a highly sensitive, yet cost-effective approach to the New Worlds Imager.

II. The New Worlds Observer

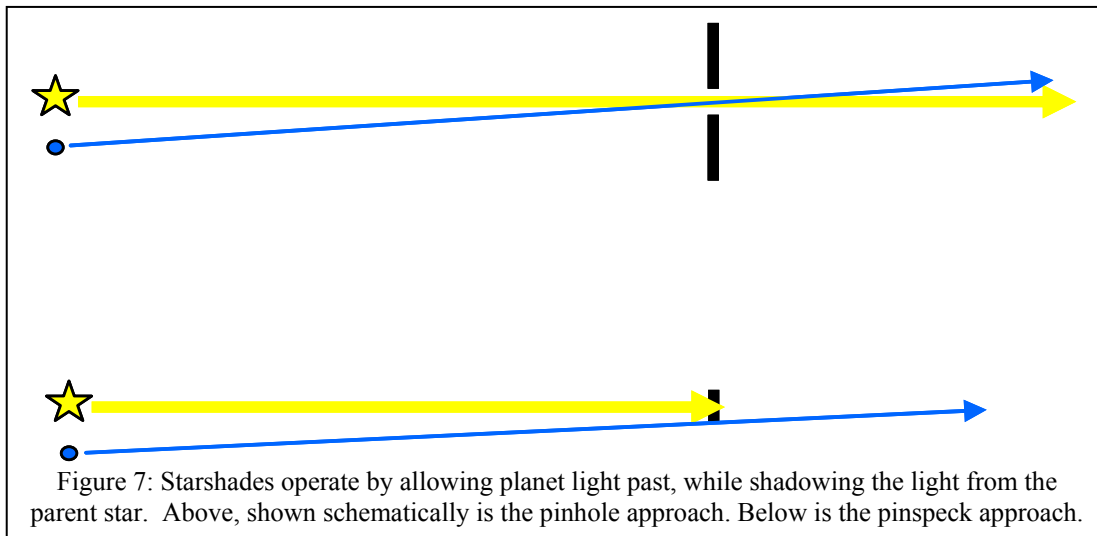
The name of this study is the New Worlds Imager, reflecting the ultimate goal of capturing actual pictures of planets. But to implement the New Worlds Imager two new technologies must be used. The first of these is the starshade for creation of high contrast and the second is interferometry across a 1000km of space. But the starshade alone is a sufficiently large step that it can create a revolution in exo-planet studies without the interferometry. We call a two spacecraft configuration (one starshade and one telescope) the New Worlds Observer (as opposed to New Worlds Imager).

In this section we discuss the development of the New Worlds Observer. We include the basics of the starshade technology and study the capabilities of the two craft configuration. We defer discussion of interferometry and planet imaging to part III.

A. Starshades

The idea of a starshade is very simple. When we instinctively raise our hands to blot out the Sun when looking at fly ball coming from that direction, we are reducing the amount of light that is entering our eyes. By reducing the amount of light that is potentially scattered, the contrast of the image is greatly enhanced. THE STARSHADE KEEPS THE STARLIGHT ENTIRELY OUT OF THE TELESCOPE.

A telescope is also capable of separating planet light from star light, but the optic must be virtually perfect to accomplish the separation with better than 10 billion to one



efficiency at a tenth of an arcsecond. Scatter from imperfections is many orders of magnitude higher. The starshade provides a low risk approach to decreasing the noise from the parent star.

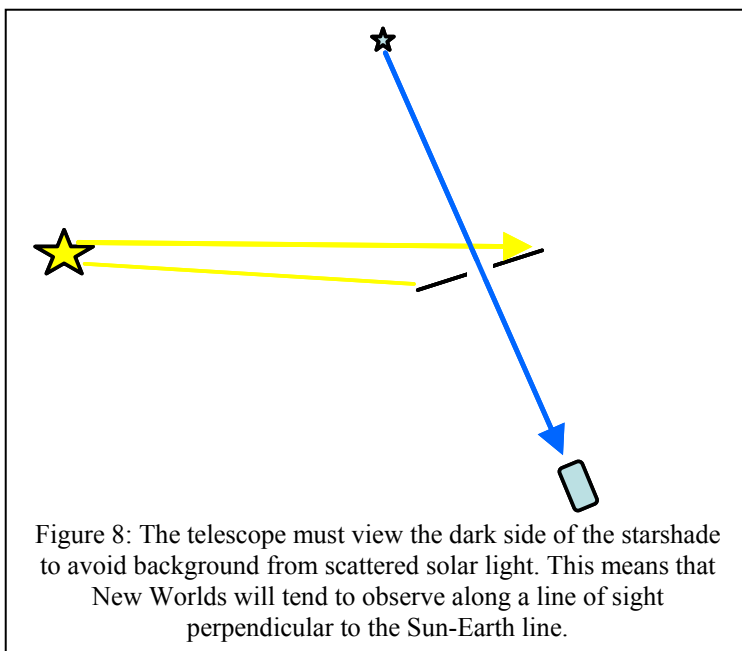
We have fundamentally two approaches to the star shade as shown in Figure 7. The first is the pinhole camera. This takes a large shade, hundreds of meters across to blot out not only the central star but the planetary system as well. The lens of the pinhole camera is a carefully shaped hole in the middle. The telescope can only see one planet at a time.

The pinspeck is an occulter. An opaque shape is moved between the telescope and the target. If properly sized and positioned it will cover the line of sight to the star but not to the planets. The difficulty has been the diffraction of starlight around the edges of the pinspeck.

At the start of this study, we assumed that the starshade would be a pinhole, because, not only was the pinhole lens perfect, the Princeton group had shown that shaping the aperture would lead to excellent suppression of diffracted light. It was pointed out by the Northrop-Grumman group that the size of the pinspecks allowed a much lighter, less expensive approach, and suggested we revisit the logic of the pinspeck. The next most obvious advantage of the pinspeck was clearly the sensitivity. Since the entire planetary system could be viewed at once, the telescope could be much smaller. A disadvantage was that the telescope had to have somewhat higher resolving power.

The pinspeck concept that emerged from this study resembles the Big Occulting Steerable Satellite (BOSS) concept described by Copi and Starkman (2000). They emphasized use of the occulter to improve spatial resolution on various kinds of targets. But they also discussed using it to blot out a star and reveal planets. They showed, correctly, a simple shape like a circle or a square would lead to 1% diffraction into the dark hole. Simple apodization did no better than 10^{-4} , a full factor of a million short of the requirement.

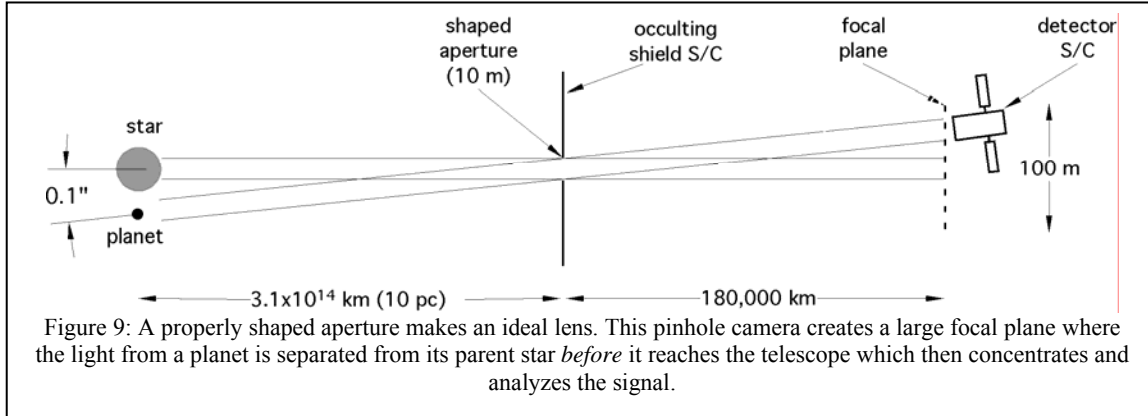
As will be explained in Section IID, we solved the problem of shaping the pinspeck so that it would reach beyond 10^{-10} contrast across a broad spectral band in a practical geometry.



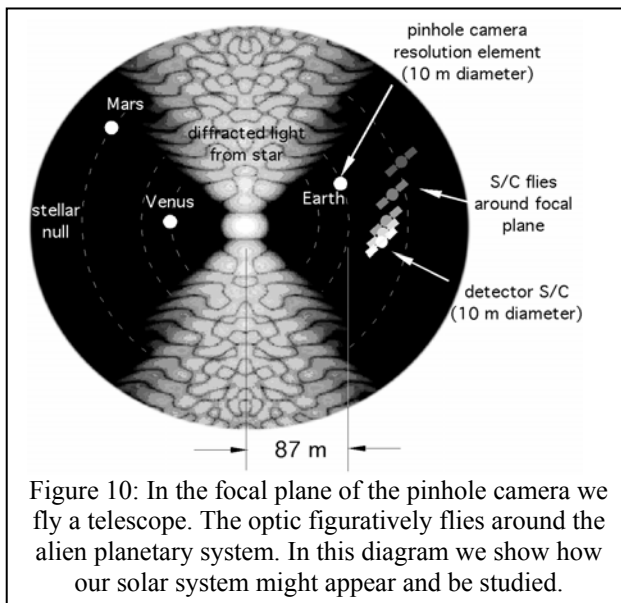
The starshade must be dark. Even our darkest materials have some level of reflection. Thus the starshade must always be oriented such that the detector craft observes the side that is out of the sunlight. Furthermore, the edges must be designed to produce a minimum of solar light scattering. This means that the starshade will usually be deployed just inside the plane defined by the perpendicular to the Sun-Earth line. Figure 8 shows this geometry. One would typically observe a star twice per year.

B. The Pinhole Camera

The basic idea for starlight rejection using a pinhole is shown in Figure 9. Two spacecraft are launched together into a high, stable orbit where they are deployed. The first spacecraft unfurls as a large umbrella of thin, opaque, dark material hundreds of meters across. At its center is an open



aperture, carefully designed to suppress diffraction. The starshade thus functions as a large pinhole camera which creates a high quality image of the planetary system many kilometers away

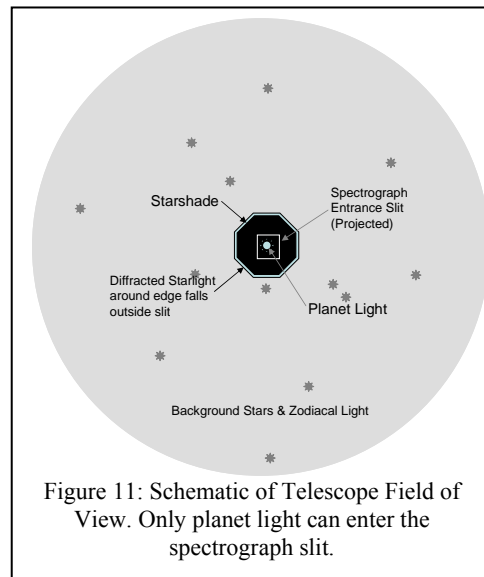


Now the Earth at 10pc is 0.1" from the parent star, so if Earth is to be 10 diffraction widths from the star and well outside diffraction, the resolution of the pinhole must be .01". This implies that the pinhole must be $2 \times 10^7 \lambda$ across, or 10 meters in the case of yellow light. Then, to create geometric separation at the diffraction limit, the focal plane must be 2×10^7 apertures away, or about 200,000km. The two craft must then hold this formation to better than a meter of tolerance relative to the line of sight.

The detector craft carries a Cassegrain telescope that focuses all of the light from the planet onto a

and a hundred meters across. The second craft carries the detector and must align with the target star at the specified distance. To acquire a planet it literally flies around the planetary system as shown schematically in Figure 10.

The use of a pinhole camera forces the detector to fly a large distance from the starshade, but the pinhole is crucial. A pinhole lens creates zero distortion to the wavefront, creates no non-uniformity of transmission and has no dust or cleanliness issues. It is the perfect lens.



spectrograph slit. We calculate that the primary mirror must be close to 10m in diameter if we are to capture the required signal in a reasonable period. Thus, depending on launch craft, the mirror may also have to deploy in orbit. Luckily, this does not have to be a diffraction-limited optic. One arcsecond should suffice, as that is a reasonable size for the shade to subtend. As shown in Figure 11, the Cassegrain views the distant umbrella, and focuses an image of the starshade. Thus the only light collected is from a single point in the target planetary system. Zodiacal light and other backgrounds are reduced to the level of a 0.01 arcsecond quality telescope, even though our telescope needs only 1 arcsecond resolution.

C. The Pinspeck Camera

The Pinspeck Camera operates in an analogous way. The occulter is 20 to 150m in diameter and flies in formation 20,000 to 200,000km from the telescope. On the focal plane, where the telescope sits, there is a dark hole cast by the pinspeck as shown schematically in Figure 12. The telescope must be maneuvered into that hole and remain there for the duration of the observation.

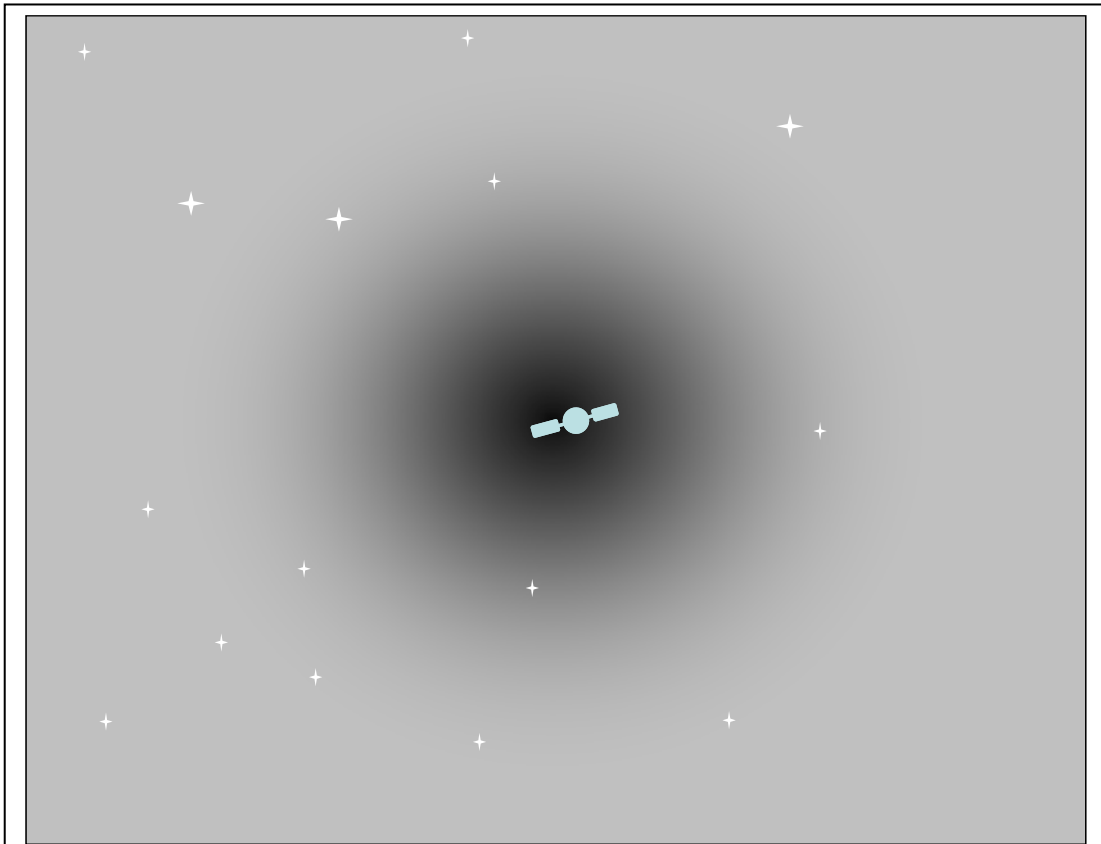
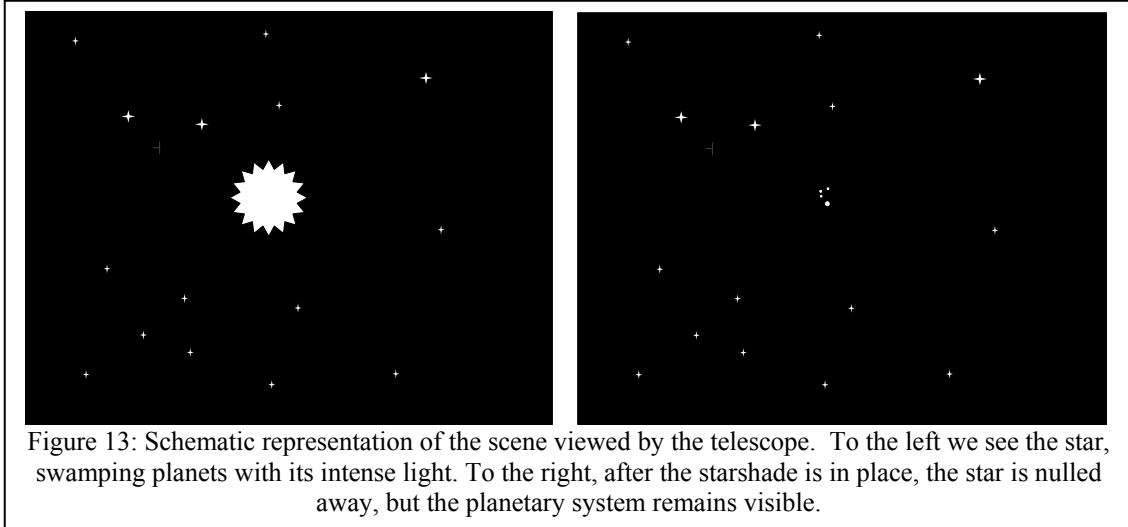


Figure 12: The pinspeck starshade projects a dark hole many meters across wherein light from the parent star is highly suppressed. The spacecraft must be flown into that hole and held there during the observation

As it moves from outside the hole into the center of the hole, the view of the planetary system changes dramatically. Figure 13 illustrates this effect. Before the pinspeck is aligned (i.e. before the telescope is fully in the shadow, the view is of an overpoweringly bright star with scattered light all over the field of view. Once inside the hole the star disappears completely, leaving only the planets.

The planets can now be studied by the conventional techniques developed by astronomers for the study of faint stars. Long term imaging of the system will show changes in brightness of all the planets simultaneously as their features rotate in and out of our sight. Spectroscopy can be performed on planets by placing a spectrograph slit at the correct position.



D. Diffraction Control

Detection of extrasolar planets is greatly hindered by the dominance of starlight in a planetary system. Successful searches require high contrast imaging with the starlight suppressed to 10^{-10} over a relatively large area of the image plane and across a broad spectral band. One such system is the proposed New Worlds pinhole camera system which employs a starshade with a shaped aperture. The starshade controls diffraction of the starlight, permitting a high contrast region that coincides with the off-axis positions of planets in the habitable region (~ 1 AU) around the star.

The pinhole system suggested for the New Worlds Observer reaches a very high limit of performance. Since there is no scatter from optical imperfections, the main limit is set by diffraction of the central star which swamps the signal from the planets. Apodized pupils can be used as diffraction control. The shaping of the pupils allows control over the beating of the different Fresnel diffraction zones. This permits manipulation of destructive interference leading to optimal suppression of the starlight.

Recent work has been conducted to determine the feasibility of an occulter or a “pinspeck” device. By exploiting the complementary behavior of diffracting screens via Babinet’s principle, we can model the occulter easily by inverting the well understood solution for the pinhole.

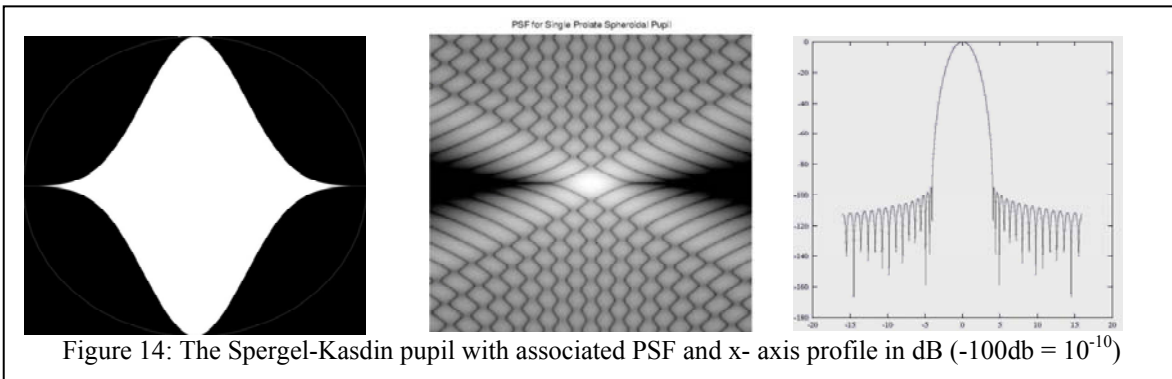
1. Pinhole

The habitable zone of a planetary system at a distance of 10 parsecs subtends an angle of 0.07 arcseconds to 0.15 arcseconds. The Earth in such a system would lie 0.1” from the parent star. To properly resolve the system, a nominal resolution limit of 10 diffraction lengths is required. At a visible wavelength of 550 nm, a diffraction limited aperture has to be larger than 10 m to achieve 0.01” resolution ($\text{Resolution} = \lambda/D$). To create geometric separation at the diffraction limit, the pinhole focus plane must be

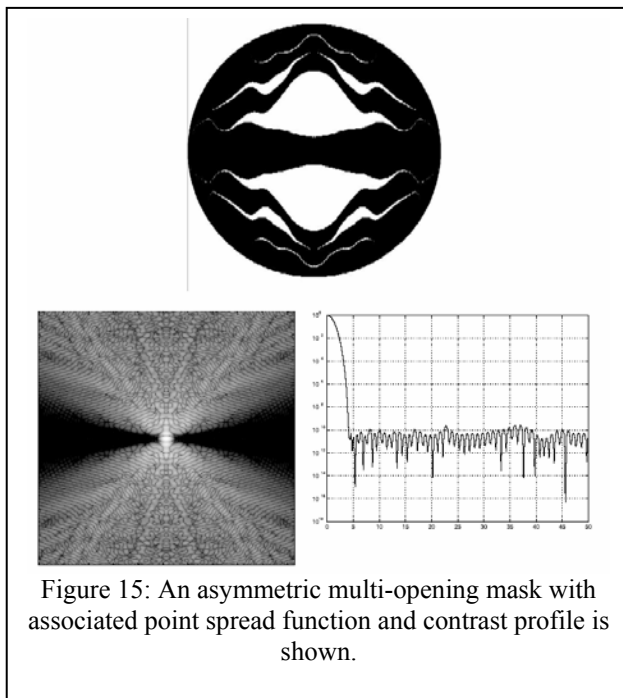
placed at the crossover between geometrical and diffraction limits. Thus the size of the aperture also determines distance to the image plane, f (Resolution = D/f). So for a 10m class aperture, we may expect the image plane to be placed about 180,000 km away.

A 10 meter class telescope orbiting a 100 meter class discovery region on the focal plane can acquire the planet signal within reasonable integration times. The ability to generate a broad region of suppressed starlight, within which the detector spacecraft may be placed, becomes crucial.

Spergel was the first to realize that shaped pupils could be used to achieve nulls of essentially any depth close (but not arbitrarily so) to the central star, and that such an idea could be useful for TPF. His first suggestion was to use a Gaussian-shaped mask. Shortly thereafter, Kasdin optimized this idea and discovered that Slepian's prolate-spheroidal



wavefunction is the optimal shape for achieving high-contrast along one axis of the image plane. This pupil mask is shown in Figure 14. It achieves a contrast of 10^{-10} everywhere along the x-axis except within $4\lambda/D$ of the center of the Airy disk.



through the pupil and around the outer edges and ensure high contrast where the planet image is expected.

Of course, the apodizations derived above assume that the opaque part of the mask extends to infinity. In reality, the mask will be a large, but finite, umbrella. The starlight will diffract around the outer edges of this umbrella. This effect must be taken into account. If one considers just a hard outer edge, then the diffraction will behave like a conventional pupil. In order to ensure high contrast at the planet location it will be necessary to make the umbrella about 100 times larger than the pupil at its center. But, if the edge is apodized (or, in the 2-D case, shaped), then one can expect to be able to use a much smaller mask - probably in the 5 to 10x range. 2-D umbrellas may be designed so as to simultaneously control the diffraction

The issue of diffracted light suppression has been previously addressed by Spergel and Kasdin. Initial aperture shapes were determined by optimizing a Gaussian mask to generate Slepian curves. This prolate-spheroidal mask achieves high contrast along the x-axis.

To widen the discovery zone where the starlight is suppressed below 10^{-10} , asymmetric multi-opening pupil masks can be considered (e.g. Figure 15). These masks are solutions to nonlinear optimization problems where throughput measures (such as open area in the mask) are maximized subject to constraints to ensure high contrast.

The shape of the aperture allows the positive and negative zones to beat against each

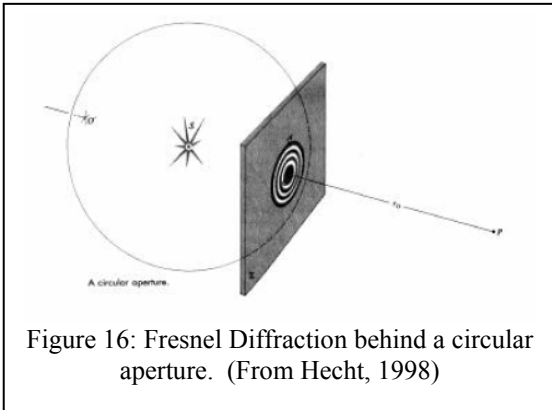


Figure 16: Fresnel Diffraction behind a circular aperture. (From Hecht, 1998)

other to suppress the diffraction from the star. Masks with sharp edges that open up in the middle, a common feature of the optimal apodization, allows a gentle introduction of the Fresnel zones. The proper shaping of the aperture allows enough zone area to enter along the leading edge to compensate for the zones lost along the trailing edge as the observer moves off axis. This smoothes the response of the PSF, allowing for broad spectral response.

The shape of the masks is sensitive to the beating of the off axis zones (Figure 16). Even though the system is effectively in the Fraunhofer regime, the size of the aperture is comparable to the size of the first Fresnel zone. In this regime, the width of the central bright spot is intrinsically determined at $4\lambda/D$, making suppression within this region effectively impossible. There are not enough Fresnel zones included within the aperture to allow for stable destructive interference and suppression. The problem of inadequate number of zones diminishes as off axis elements come into play. As observation positions depart from the central axis, the Fresnel zones

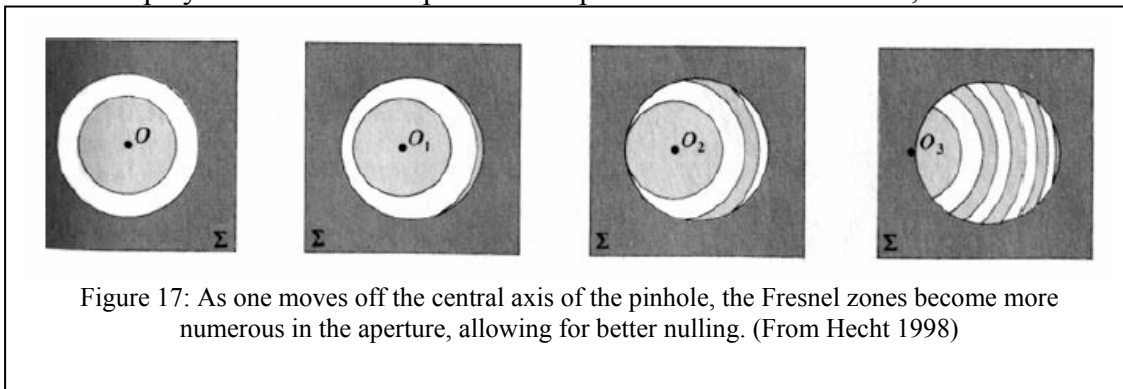


Figure 17: As one moves off the central axis of the pinhole, the Fresnel zones become more numerous in the aperture, allowing for better nulling. (From Hecht 1998)

in the updated field of view are narrower in width. This allows multiple Fresnel zones that surround the main Fraunhofer band to fill the aperture, as shown in Figure 17. In the panel on the left, the aperture covers exactly two zones leading to suppression through destructive interference. As the observation point moves off axis, the observed intensity begins to oscillate. The total optical disturbance is the sum of the visible zones in the aperture.

The optimization condition for a pinhole camera employs the Fraunhofer formula to determine the electric field at a point ξ on the image plane. So for an aperture of radius $D/2$, the electric field optical disturbance on the image plane is given in one dimension by

$$E(\xi) = \int_{-D/2}^{D/2} e^{ik(\sqrt{f^2 + (\xi-x)^2} - f)} A(x) dx$$

Where f is the distance to the image plane and $k = 2\pi/\lambda$ is the wavenumber. To derive the above Point Spread Function (PSF, optical disturbance vs image plane), we determine the apodization function $A(x)$ through the following optimization:

$$\begin{aligned} \text{Maximize} \quad & \int_{-D/2}^{D/2} A(x) dx && \text{(Throughput maximization)} \\ \text{Subject to} \quad & |E(\xi)| \leq \mathbf{10}^{-5} |E(0)| && \text{(High contrast condition)} \end{aligned}$$

Circularly symmetric apodization functions such as the starshape mask have also been analyzed. The starshape mask is characterized by the set S in polar co-ordinates given by

$$\begin{aligned} S &= \left\{ (r, \theta) : 0 \leq r \leq \frac{1}{2}, \theta \in \Theta(r) \right\} \\ \Theta(r) &= \bigcup_{n=0}^{N-1} \left[\frac{2\pi n}{N} + \frac{\alpha(r)}{2}, \frac{2\pi(n+1)}{N} - \frac{\alpha(r)}{2} \right] \end{aligned}$$

Where r and θ are co-ordinates in the aperture plane and $\alpha(r)$ is the width in radians of a spoke in the starshape mask.

The electric field in two dimensions can be written in polar co-ordinates as

$$E(\rho, \phi) = \iint_S e^{-2\pi i \rho \cos(\theta - \phi)} r dr d\theta$$

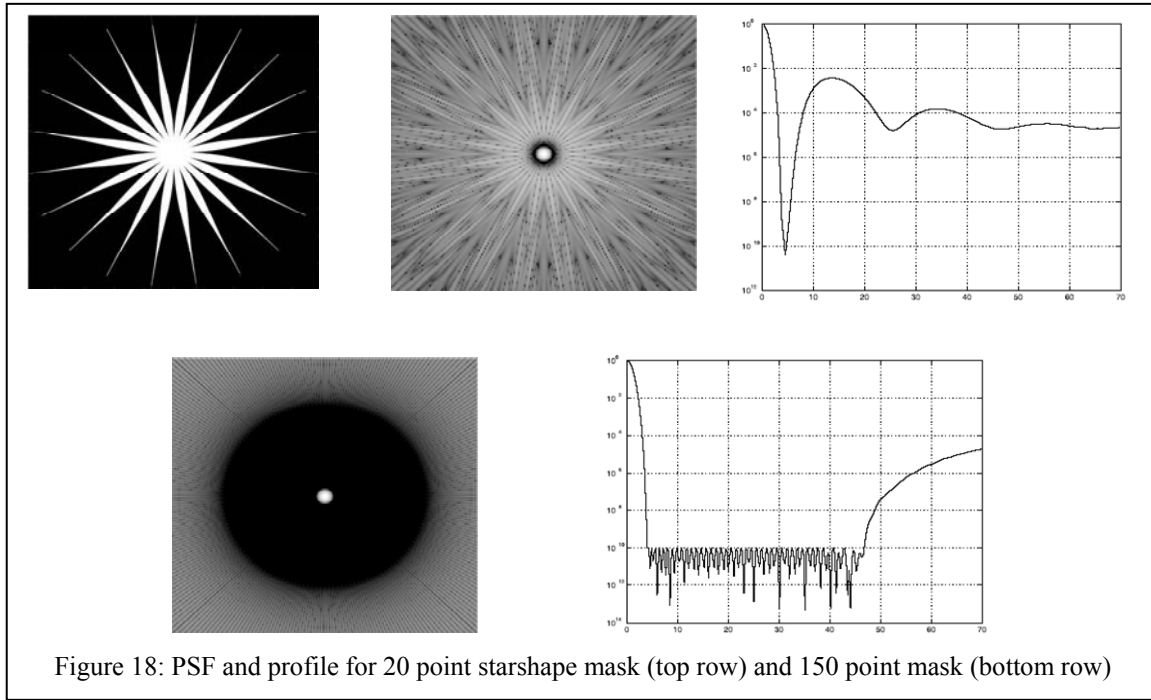
where ρ and ϕ are the radius and angle on the image plane. The radii are stated in dimensionless units where r is given as a multiple of the aperture D and ρ is a multiple of the focal length times the wavelength over the aperture ($f\lambda/D$). The integral for the optical disturbance can be expressed in terms of Bessel function solutions; simplified to terms relating to the zeroth order Bessel function (J_0) and terms with higher order Bessel functions that correspond to the number of spokes in the starshade mask. With a large number of spokes the higher order Bessel terms become negligible at small ρ , allowing us to ignore all but the zeroth order Bessel term. (The details of this process are worked out in Vanderbei, Spergel & Kasdin, 2003 hereafter VSK). Thus the symmetry of the problem and the characteristics of the starshape mask permit the equation to be rewritten as

$$E(\rho, \phi) = \int_0^{1/2} J_0(-2\pi\rho) [2\pi - N\alpha(r)] r dr$$

Noting the similarity of the above equation to the general circular aperture solution with apodization, the following relationship between the shape function of the spoke $\alpha(r)$ and the apodization function $A(r)$.

$$\alpha(r) = \frac{2\pi}{N} [1 - A(r)]$$

The above equation is extremely versatile in allowing the optimization of standard apodization throughput. The derived optimal apodization transmission function in one dimension can be used to shape a binary mask that yields the same PSF when extrapolated to the 2-D image plane.



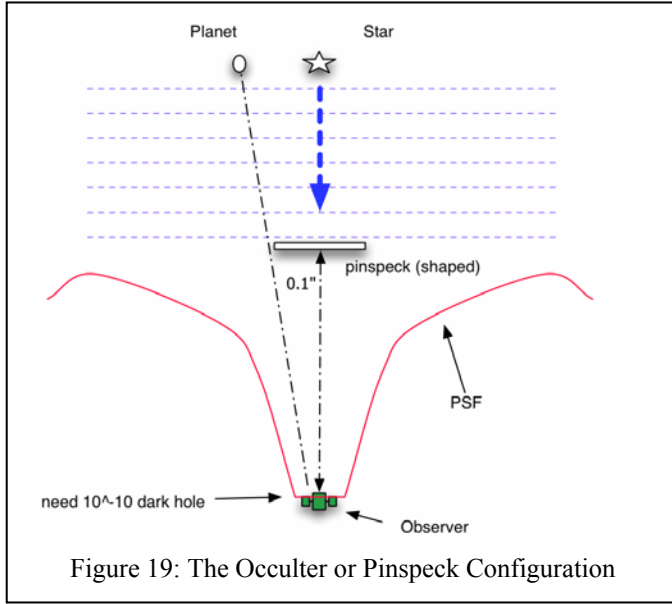
The optimal apodization problem is similar to the one done in Cartesian co-ordinates where the throughput is maximized subject to a constraint ensuring high contrast. For a viable starshape mask solution, various smoothness constraints are also needed. Motivated by the similarities to Gaussian solutions of many optimal apodization, the following smoothness constraints are also implemented. The resulting PSF functions are shown in Figure 18.

$$\begin{aligned} \text{Maximize} \quad & \int_0^{1/2} A(r) 2\pi r dr && \text{(Throughput maximization)} \\ \text{Subject to} \quad & |E(\rho)| \leq 10^{-5} |E(0)| && \text{(High contrast condition)} \\ & 0 \leq A(r) \leq 1 && \text{(Smoothness Constraints)} \\ & dA/dr \leq 0 \\ & A(r) d^2A/dr^2 \leq (dA/dr)^2 \end{aligned}$$

We have affirmed through numerous simulations that a broad high contrast region can be obtained for the pinhole camera New Worlds Observer.

2. Pinspeck

To assure that diffraction from the edges of the starshade does not affect the characteristics of the aperture, a large starshade needs to be deployed. This drives up the cost of the project. Similar goals and contrast levels may be achieved through the complementary aperture under Babinet's principle. Thus an occulter or "pinspeck" camera, where an obscured diffraction sheet sits in an infinite open plane, becomes an economical way of reaching mission goals (Figure 19).



Thus an occulter or "pinspeck" camera, where an obscured diffraction sheet sits in an infinite open plane, becomes an economical way of reaching mission goals (Figure 19).

The occulter requires the system to take advantage of Fresnel behavior. In the Fraunhofer regime, the occulter does not cover enough Fresnel zones to allow for zone beating effects. A null at the center of the

system in Fraunhofer configurations cannot be achieved as the occulter does not cover more than one zone. Furthermore, the bright spot at the center in the Fraunhofer regime cannot be shrunk to more than a few λ/D . As demonstrated in the pinhole studies, the telescope must move to $4\lambda/D$ just to allow nulling to occur in the high contrast region. Fresnel conditions imply that occulters obscure many zones allowing for broad regions of stable high contrast both off axis and across wavelengths. The shape of the occulter is carefully chosen to include the same number of zones at the leading edge as are revealed by the trailing edge moving off the Fresnel pattern in an off-axis shift. Similarly, a change in wavelength simply scales the widths of the Fresnel zones. The shaped masks should be able to account for the change by compensating for zone loss with wavelength change.

The analysis used to determine optimal apodizations for the Fraunhofer regimes is easily adapted to Fresnel. Because the approximation that $F \gg D$ can no longer be made, the electric field integral acquires an extra exponential factor solely dependant on r , the radius on the aperture plane.

$$E(\rho, \phi) = \int_{1/2}^{\infty} J_0(-2\pi r \rho) e^{-ikr^2 D^2/F} A(r) r dr$$

To make the electric field integral tractable, the complementary behavior of apertures may be exploited. Babinet's principle states that optical disturbance from two

complementary apertures add to the unobstructed electric field as the limits of integration of the open area go to infinity ($E_1 + E_2 = E_0$). Thus to determine the optical disturbance from the occulter, the solution for the aperture can be subtracted from the undisturbed electric field. The solution then becomes

$$E_{occulter} = E_0 - \int_0^{1/2} J_0(-2\pi r \rho) e^{-ikr^2 D^2/F} A(r) r dr$$

The integral part of the above solution can be written as a complex number with C signifying the constant derived from the cosine integral and S the constant from the sine integral. All graphs of interest require 10^{-10} contrast in irradiance which is simply the optical disturbance squared. So that the quantity

$$I = \left(1 - \sqrt{C^2 + S^2}\right)^2$$

must be less than 10^{-10} in the region of interest.

Figure 20 is a plot of Airy disk profiles for circular apertures in the Fraunhofer regime. The first two panels represent the disk in normal and logarithmic units. The last panel is the standard airy solution for the pinhole aperture Babineted to obtain the solution of the complementary occulter. As the figure shows, the dark region in the center, though not broad, can achieve nominal contrast of 10^{-7} even without optimization. This motivates the

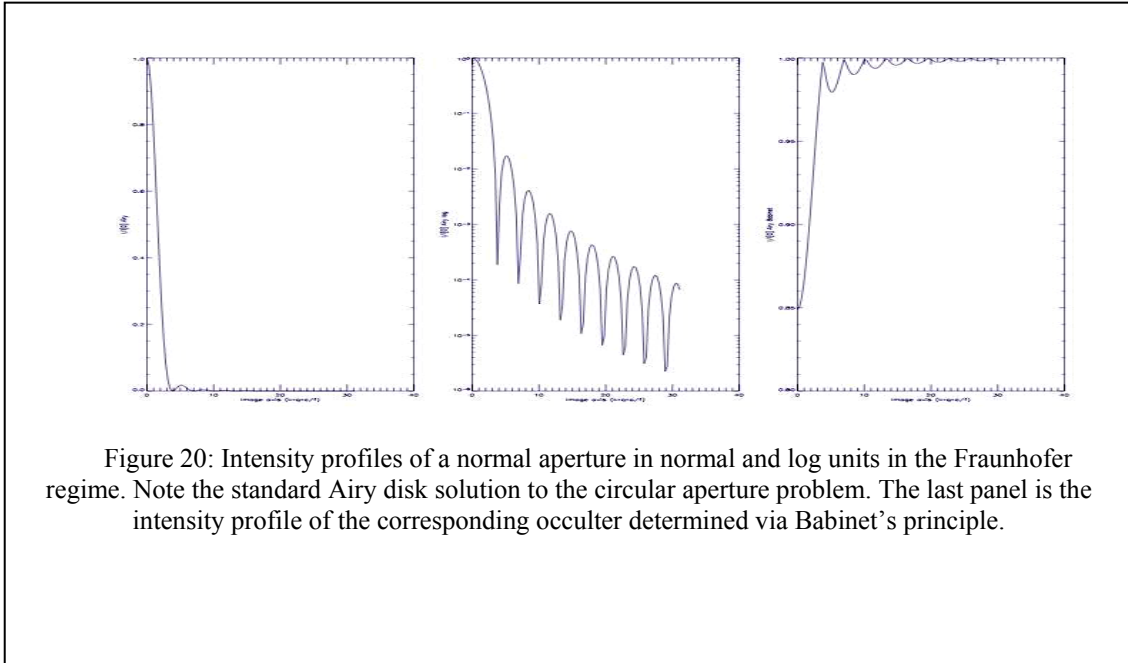
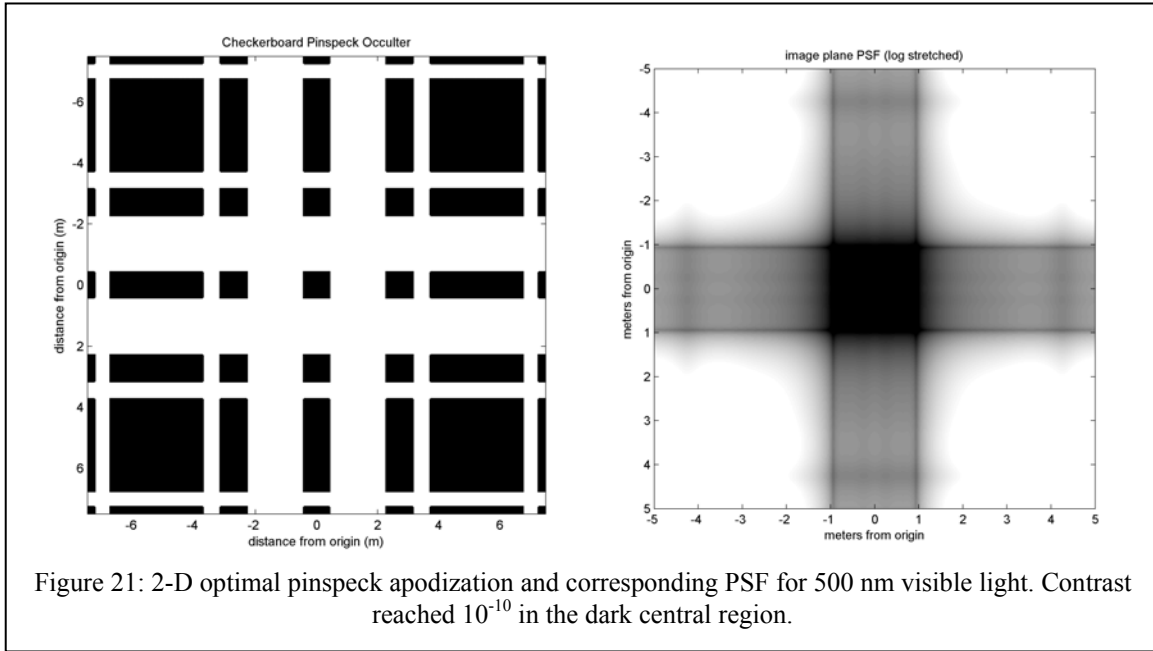


Figure 20: Intensity profiles of a normal aperture in normal and log units in the Fraunhofer regime. Note the standard Airy disk solution to the circular aperture problem. The last panel is the intensity profile of the corresponding occulter determined via Babinet's principle.

use of occulters to create high contrast regions near the axis. Our simulations adapt the tractable Fraunhofer solution to the Fresnel regime of the occulter and seek stable and robust solutions across wide wavelength bands.

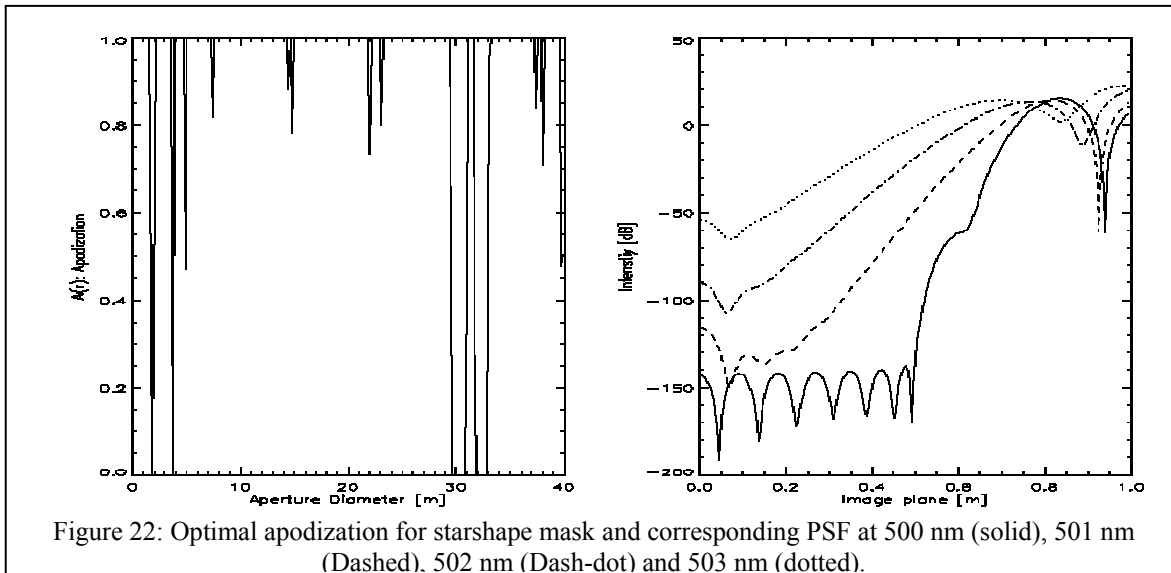
Initial attempts sought to perform a rigorous two dimensional array approximation of the apodization on the aperture plane. The irradiance was determined by direct

integration over all light paths at various off axis positions. This method is very computationally intensive. Furthermore, the resolution required to model smooth edges of the shaped occulter made memory requirements impractical. Nevertheless, contrast regions of 10^{-6} were easily achievable. The solution was too imprecise to subject to rigorous testing over wavelength or attempt to optimize the size of the high contrast



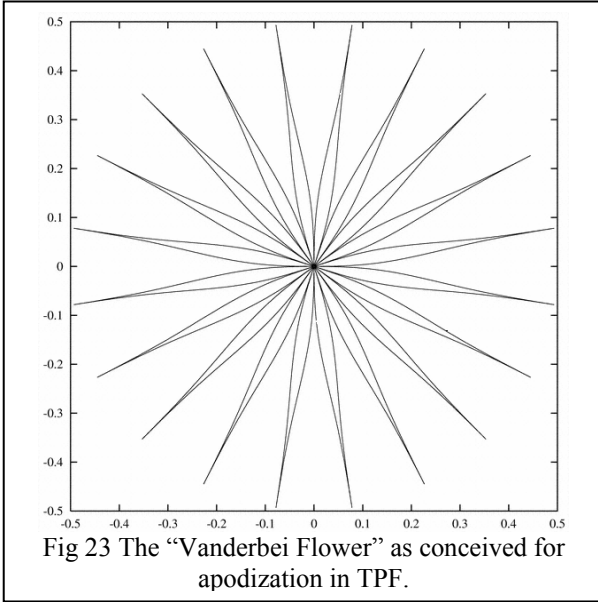
region.

In order to simplify computational methodology, separable solutions around specific axes were considered. This converted the Fresnel conditions into one-dimensional integrals. To ensure easy construction, the apodization was further constrained to only return binary values separating the mask into dark and light regions with no partial transmissions. The optimization problem mirrors the Fraunhofer optical disturbance equation with an extra complex exponential factor solely dependant on x (displacement in the aperture plane). At a given wavelength the optimization problem and constraints are linear, so a global optimal solution must exist. To find such an optimum we formulate a non-linear, non convex problem with the 1-D apodization as a starting point. This returns



the optimum position of the dark regions giving us a 2 dimensional checkerboard pattern as seen in figure 21.

The rectangular solutions are poorly suited to the naturally spherical nature of the incoming light wave. For this reason, such solutions are extremely difficult to achieve and perhaps not as robust as their circularly symmetric counterparts. In an attempt to



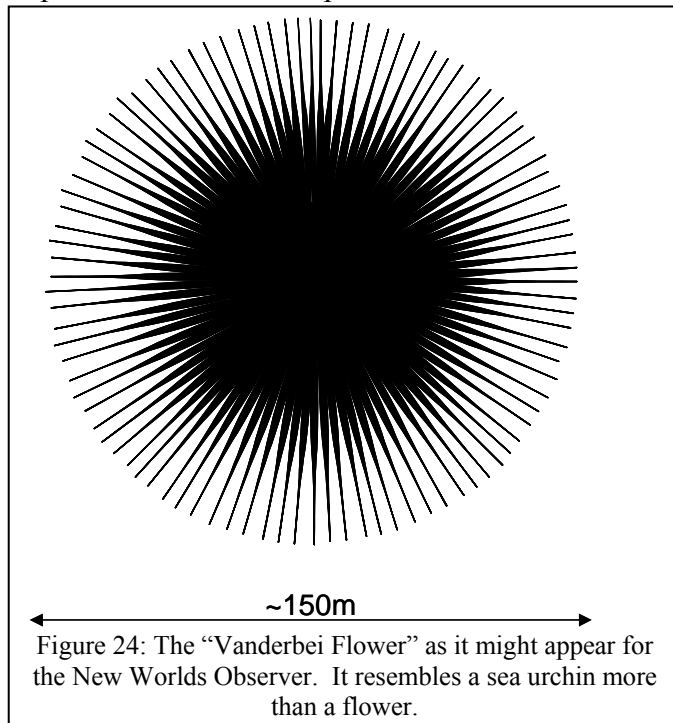
determine circularly symmetric solutions that would also be viable for practical construction, the starshape mask solution is adapted to the Fresnel occulter regime from the pinhole problem. As with the Cartesian 2-D solution discussed earlier, the Fresnel integral is simply the Fraunhofer one modified by a complex exponential factor which is solely dependant on the radius on the occulter plane. The same linear programming pipeline used to determine solutions in the separable 1-D problem can be adapted to solve the circularly symmetric problem.

Since the Fresnel integral does not depend on the azimuth angle, we extrapolate the same symmetry arguments

to remove the azimuthal dependence because of its relationship to high order Bessel terms. The linear optimization function will return an apodization which, while not necessarily binary, determines the shape of the individual spokes in the starshade mask because of the relationship between the shape function $\alpha(r)$ and the apodization.

A sample solution is shown in figure 22 for an occulter 80 meters in diameter with an image plane placed 20,000 km away. The apodization function reveals an antenna like structure for each spoke. However, the solution is only robust in one wavelength and quickly collapses as deviations of 1 nm are introduced.

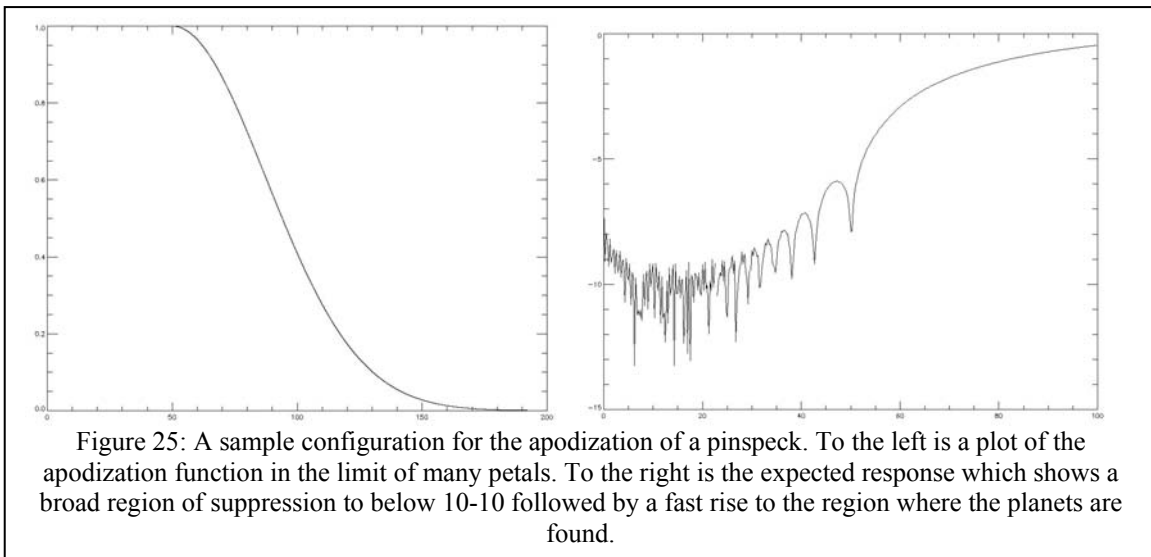
At the end of the Phase I study we finally found a pinspeck design that both meets the contrast requirements and is small enough to launch. The design is based on the work of Vanderbei, Spergel and Kasdin (2003). They



showed a flower-like shape (see Figure 23) could be used as an aperture to create a pupil that allows high transmission in the center and a fast falloff to high contrast in all directions around the central spot. This shape is a prime candidate for use in a pinhole camera.

It occurred to us that such a shape might work well as an occulter if it were made sufficiently large to cover the central (Fraunhofer) zone. After some searching we found just such a solution. Shown schematically, in Figure 24, it consists of a dark central zone, with spines (or petals) that taper slowly outward. The number of petals shown is 96, but optimization of the design may reduce the required number.

Numerical evaluation of a somewhat larger example is presented in Figure 25. In this case our central obscuration is 100m diameter, with the petals falling to half width at 140m diameter. The thin (low mass) ends of the petals taper out past 300m diameter. The occulter is 200,000km from the telescope. So, this is a large occulter, but it is sufficiently



small to be launched by a single rocket and deployed at L2.

When the Fresnel integrals are evaluated across this shape with an apodization function as shown in Figure 25 (a), then the diffracted light follows the profile shown in Figure 25 (b). The contrast is below 10^{-10} across a large (nearly 100m) diameter. The diameter is so large that any planned telescope can be easily fit within. Equally important, the contrast rises to above 10^{-1} at the position of the Earth, so the planets are not simultaneously occulted. This behavior persists across a wide band of the spectrum. It works even better in the ultraviolet as short as Lyman α (1216\AA). As the wavelength moves longward of a couple microns the contrast starts to drop as the longer wavelengths no longer interfere against each other completely.

This particular design is simply an example that proves the pinspeck cameras will work and are practical. We expect that optimization will allow us to shrink them substantially. That work is ongoing.

E. Starshade Deployment

An occulter has two major characteristics – a circular exterior and multiple radial members. Deployment of such a device consistent with packaging in a small fairing could

be performed in at least two ways with direct heritage to proven deployable designs and commensurate high TRL (TRL>6). The two methods are;

1. The petals of the flower can be pulled outwards and tensioned by creating a circular structure around the outside of the occulter,
2. The flower petals can be pushed out by an array of telescoping linear actuators

Both of these approaches can be accomplished using high TRL level hardware as described below.

A circular structure can be developed from the flight-proven Astromesh perimeter truss reflector. These type of structures have been flown successfully on four major commercial missions to date. The perimeter truss structure is shown in various stages of deployment in Fig 26 below. In the figure it is shown drawing out an arrangement of webs and mesh to form a reflector surface. In the concept the occulter legs would replace the webs and mesh. The legs could be made of a flexible frame with a membrane stretched across it. The frames would fold up within the perimeter truss in the same manner as the webs.

The AstroMesh perimeter truss is a well-proven mechanical device that is deployed by cable spoolers driven by either stepper or D.C. motors. In the concept, the spacecraft would be suspended in the middle of the occulter much like a spider in its web. Structural models have been created of this type of configuration for RF reflectors and have been

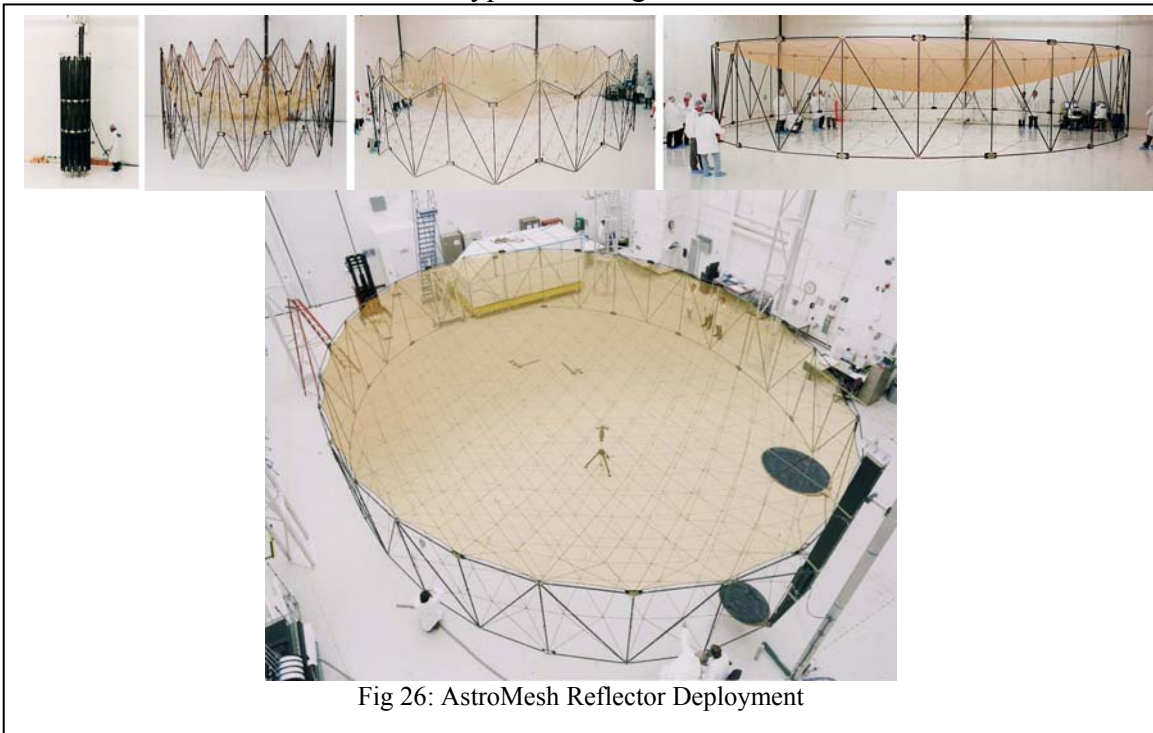


Fig 26: AstroMesh Reflector Deployment

shown to give very good dynamic performance.

For a radial deployment a different mechanism is required. A candidate for this is the telescopic tube which has been developed at Astro. The design has been qualified for the NASA ISIS (Inflatable Sunshield in Space) program and has been developed in various sizes on IRAD programs as shown below.

The concept for a small 7.5-meter occulter above is that a fan array of 20 telescopic tubes would be arranged around a central drive hub. Each tube would collapse to 20

inches long and would be 5 inches diameter. They would fit around a 30-inch hub providing a stowed package of 70 inches diameter that would fit a small launcher shroud. The legs of the occulter would be of the same construction discussed above, the tip of each leg would attach to one telescopic, and it would also be attached to some of the telescopic sections along its length. As the central drive is actuated the 20 tubes would



Figure 27: A space-rated deployment mechanism developed by Astro.

deploy and pull the occulter into position.

The Phase I study has shown that an occulter, as shown in Figure 24, will provide sufficient contrast for planet imaging. The challenge therefore is to build a precision deployable structure for the allowed weight, mass and volume constraints. It will be a main effort of a Phase II study to understand the factors that allow the occulter size to be

decreased, and combine this with the need to meet weight and station keeping requirements.

There are a number of potential solutions, for the overall architecture of the occulter craft, allowing for a right trade study to be performed in Phase II. The completely obscured central area is an ideal location for the spacecraft, housing propulsion, navigation, location aides, command and data handling and other usual space craft systems. This spacecraft can be realized in a number of ways from a small volume suspended in the middle like a fly in a spiderweb, to being rigidly mounted to a frame that is the foundation of the deployed flower.

Deploying out from the central obscuration, the petals of the flower are a precise deployable. These petals are long and thin, and there are various methods of deployment that exist for study and trade. The first family of options is use of a rigid set of deployables that either pull or push the petal into place. The petals can be pulled outwards and tensioned by creating a circular structure around the outside of the occulter. The petals can also be pushed out by an array of telescoping linear actuators

These type of structures have been flown successfully on four major commercial missions to date. The perimeter truss structure is shown in various stages of deployment in Fig 26. The legs could be made of a flexible frame with a membrane stretched across it. The frames would fold up within the perimeter truss in the same manner as the webs.

The petals can be also be deployed from a central hub, the analogy would be a powered antenna similar to those found on automobiles, save there would be many driven from a central motor.(Figure 27) The petals could also be deployed using a tape deployment, where a linear spring is coiled and then released, allowing the petal to unroll. Both the direct booms and tape mechanisms have been used successfully on previous flights and are of high TRL.

Another element of the trade study should be the option of making a precision inflatable structure that can be rigidized. This technology is being developed on other programs, such as DARPA's ISAT program, and offers the promise of very low areal density structures.

Another potential set of options to be included in the Phase II study are hybrid designs, where some aspects use driven deployable and some are inflatable.

The study would begin with a model of the occulter, so that the optical performance in terms of contrast ratio and the like could be calculated for each design. This would allow the evaluation of how specific features of the designs, such as an out ring from and Astromesh based design, would impact performance. Also to be included will be an initial estimate of dynamic performance, mass and the ability to be packed into an available fairing. Finally the occulter deployment study will flow into a mass budget, which motivates the selection of a launch vehicle and a cost model for the occulter.

This parametric cost model is then used to identify the optimum method for deployment of the occulter petals. Furthermore, existence of such a system level tool allows for the revisitation of the launch vehicle choice and therefore program cost estimates as the optimization of the occulter proceeds.

F. Formation Flying

The crucial break with tradition that enables the New Worlds Observer is the use of formation flying spacecraft at large separations. No analog of this concept is possible from a ground-based or single spacecraft observatory. Precise formation knowledge and control is needed to reach the high angular resolution for direct exo-planet sensing. Collaborator Jim Leitch is actively involved in a detailed study of formation flying under a cross-enterprise grant. There is also active involvement in formation flying development within our Princeton and Northrop-Grumman sub-groups. It appears that the requirements of generating the knowledge of the line of sight and then holding the craft in their respective positions can be handled with techniques combining high precision celestial and inertial sensing and stabilization. During the study, the tradeoffs and optimization of the formation flying approach will be performed starting from an allocation of allowed errors amongst the key observatory subsystems. An example of the allocation and trade study process is given by consideration of the effect of pressure of the solar wind on the large, light structure of the starshade. The added image degradation due to increased motion of a larger starshade will be compared to the increased diffraction scatter from a smaller starshade to find the best shade size to use for the mission.

NWO's (and even moreso NWI's) mission requires absolute and relative position knowledge for both the detector and occulter, coupled with a robust metrology system to quantify and qualify the state of each component to aid in image reconstruction. To achieve these requirements, the system must operate in a quiescent environment where the effects of various perturbative forces can be detected, predicted and ultimately mitigated by the flight control system.

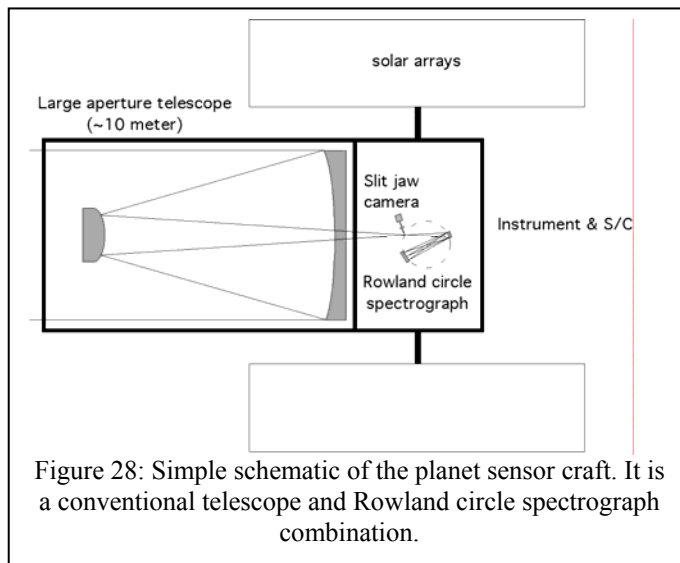
By operating at one of the Earth-Sun libration points, NWO can leverage the point's region of quasi-stability to simplify the dynamics of the system and allow for active control of each component to within 10 cm in real time across a 20,000 km focal length. From operational experience and analysis, the benefits and costs associated with maintaining a mission about each of the Lagrange points is well understood. Of the five Lagrange points, only three are viable candidates for the proposed mission. L3 is within the photosphere of the Sun, and L1, while lying between the Earth and the Sun, presents an unnecessary constraint on the visibility of the effective system by precluding targets located both sunward and towards the Earth. At L2, L4 and L5, the dominant force acting on the system is solar radiation pressure, with secondary perturbative effects due to the Earth and Moon. Of these three potential points, L4 and L5 are less attractive candidates since the influence of solar radiation pressure is greatest at these two points and when combined with the asymmetric torque induced by the gravitational attraction of the Earth and Moon, requires increased stationkeeping cycles and budgets for the objective mission life.

This is in stark contrast with the beneficial alignment between the Sun, Earth-Moon and the spacecraft at L2. This linear arrangement affords NWO with an improved visibility of target stars, along with aligning the resultant forces due to solar radiation pressure and n-body gravity. Therefore, a halo orbit about L2 provides NWO with the most benign environment to support operations both actively and passively. At L2, a preliminary analysis estimates that the delta-V required to support imaging operations is approximately half that at L4 and L5. This reduction in required stationkeeping benefits the system as a whole. With less thruster firings, the fuel mass required for NWO is

reduced, which directly translates to mass and cost savings at launch. Additionally, with smaller and more infrequent maneuvers, the control system becomes less complicated which in turn increases the system's reliability.

Injection into and operating at L2, has been successfully demonstrated by other missions, highlighting that the necessary infrastructure and knowledge base exists to support NWO. These benefits combine together directly to effectively lower the risk of NWO, while improving the operational duty cycle of the overall imaging mission. The requirements for the propulsion system can be met by either pulsed plasma thrusters or field emission electric propulsion technologies.

G. Telescope & Spectrograph



The role of the telescope is to collect the light from the target and feed the light into a photometer, spectrograph or relay optic, so the telescope need only image a very small field of view and can operate on-axis. This allows the use of simple two-element telescopes, e.g. a Cassegrain.

The resolution of the telescope is set by the size of the starshade in the pinhole case, and can be as poor as 1 arcsecond, but the increased background from scatter off the starshade

recommends resolutions closer to 0.1''.

In the case of the pinspeck camera, the telescope should be no poorer than 0.3'' because it would be unable to separate planets from each other in the inner planetary system as viewed from 10pc. A tenth of an arcsecond is approximately the diffraction limit of a one meter telescope which, coincidentally, is the minimum size needed to collect the signal. So we have chosen 0.1'' as the quality needed.

The detector used in the spectrograph must have an extremely low intrinsic background to minimize the noise in the spectrum, as the fluxes from the planet will be low.

With the basic requirements it is straightforward to estimate the required exposure times versus aperture diameter for the spectrograph. As a straw-man instrument we have assumed an instrument with a two-element telescope, and one of three moderately sized (~ 100 mm with 0.010 mm pixels) detectors; glass microchannel plates, silicon

Table 1

Diameter (m)	Required integration time (days) to get 100,000 counts	Detector Noise (counts)		
		MCP _{glass}	MCP _{Si}	CCD
1	28	363	15	604800
5	1.1	15	0.6	24192
10	.3	4	0.1	6070
15	.1	2	0.06	2700
20	.07	1	0.04	1512

Assumptions: $F_{\lambda} \sim 3e-9$ photons/cm²/sec/Å for Earth at 10pc, system efficiency ~0.35, $\lambda=5000\text{\AA}$. Background calculations done using MCP_{glass}=0.5 counts/cm²/sec, MCP_{silicon}=0.02 counts/cm²/sec, CCD=1e- read noise and readout every 20 minutes, and a 0.03x1 mm resolution element with 0.010 mm pixels.

microchannel plates, or a CCD. In addition, we are baselining a spectral resolution of 1000 across the band. We also assume a reflectivity of 90% for each reflection, a groove efficiency of 75%, a detector quantum efficiency of 80%, and an obscuration factor of 80%. These values represent either currently demonstrated performance or assume a modest increase in performance expected

as technology improves. The bandpass of the instrument will cover from 1150Å to 20,000Å, thus including potential auroral emissions from 1216Å and the major biomarkers between 5000Å and 9000Å. With these assumptions the net efficiency of the instrument is ~0.35. In reality different detectors may be required to cover the entire band-pass and there can be significant wavelength dependence in optics performance and detector quantum efficiencies, however, more detail will be forthcoming in the study.

The number of detected counts can be computed versus telescope collecting area along with intrinsic noise from the detector. Assuming the flux distribution shown in Figure 35, and a spectral resolution element .03 mm x 1 mm we calculate the telescope diameters and count rates (see Table 1).

Detector technology will play a crucial role in the instrument; intrinsic detector background can overwhelm the weak signals and force unacceptably long integration times (see Table 1). However, in the UV silicon MCPs are proving to be far superior to glass MCP detectors in their intrinsic background, due to the lack of radioisotope contamination in the silicon. Current silicon MCPs are demonstrating background rates of 0.02 counts/sec/cm² compared to 0.5 counts/sec/cm² for glass MCPs. CCD detectors are unlikely to be suitable, but CMOS detector technology is advancing rapidly and remains very promising. In any event, we will thoroughly parameterize the required detector performance characteristics and evaluate current detector technology for suitability.

H. Simulations

1. Planet Finding

The feasibility of the New Worlds missions is entirely dependant on the telescope's ability to achieve sufficient signal to noise from an exoplanet in a short amount of time. Larger telescopes allow for higher photon counting rates, while at the same time increasing resolution capability. Still, increasing apertures can drive up costs significantly, so we have studied the tradeoffs between the different proposed designs. Simulations were run to test NWO's ability to detect extrasolar planets assuming a configuration capable of 10^{10} contrast. These simulations were done for both the pinhole and pinspeck configuration observing our solar system at 10 parsecs. Integration times were studied from 50 kiloseconds (ks) to 400 ks in increments of 50 ks to see signal to noise improvement and which planets are detectable. In all pinspeck cases Mars can be easily detected in only a half day. Due to having to fly around the pinhole camera's focal plane, the pinhole configuration requires longer integration times to make the same detections as the pinspeck.

Background noise is then considered in the final sections. Visible zodiacal light scattered off interplanetary dust around the central star, as well as galaxies discovered in the Hubble Deep Field, are capable of interfering with planetary signals. The area of interest for this background is the habitable zone, where we are interested in finding terrestrial planets capable of supporting life. In both the pinhole and pinspeck configurations, zodiacal light of the central star was simulated and found to not interfere with planetary detection out in the habitable zone for face-on views of the planetary system. Deep field galaxies are of comparable brightness to exo-planets, and are on average larger on the focal plane. In the end this is actually a benefit, as their oblong shape will give away their nature, and waiting long enough for the star to pass by the galaxy allows for a clean observation of the planetary system.

PINHOLE CAMERA : The design of the pinhole camera configuration requires that the telescope orbit around in the focal plane which is several hundred meters wide located 180,000 km away from the star shade. At 10 parsecs the Earth is $0.1''$ away from the central star, but must

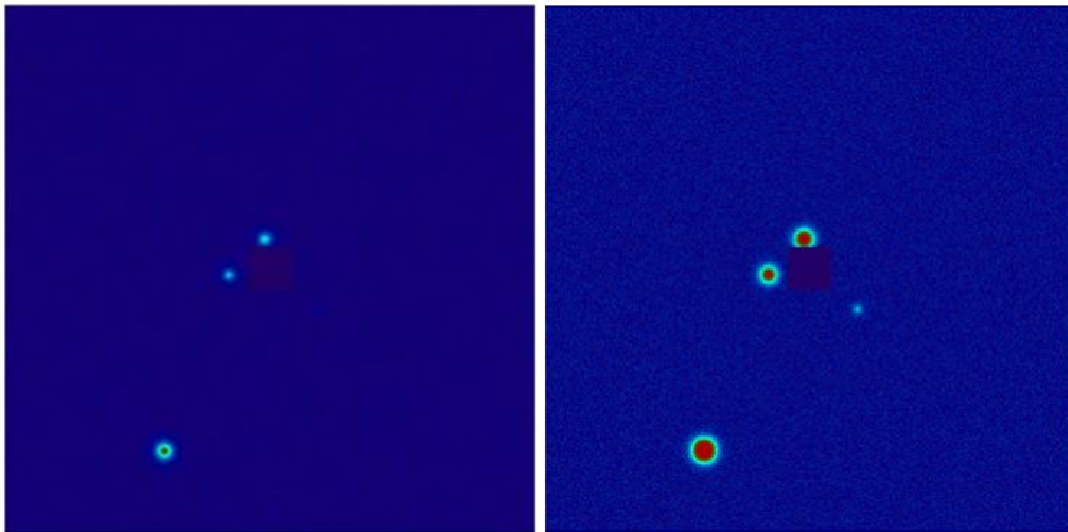


Figure 29: Simulations of the inner 6 AU of our solar system at 10 parsecs seen with the pinhole camera. To the left a half-day is spent collecting light throughout the focal plane. To the right four days are spent, and Mars is detected.

be resolved to 10 diffraction widths, or $0.01''$. To meet this requirement at visible wavelengths the pinhole must be 10 meters. The telescope diameter is set by the pinhole diameter in order to maximize light collection and effectively acts as a resolution element on the focal plane. For our simulations the images correspond to $\sim 200,000 \text{ m}^2$ in the pinhole focal plane, so it takes roughly

2500 pointings of our 10 m telescope to survey the region. Although this doesn't leave much integration time in each spot on the focal plane, this setup can accumulate 15 counts per second from the Earth, so a solid detection only takes ~ 7 seconds. It is assumed that the 50 ks of detection time does not include time for maneuvering the telescope around the focal plane. However, realistically, the telescope will collect light as it circles through the focal plane.

The central region is not surveyed, since the diffraction pattern cannot suppress starlight any closer to the star than $4\lambda/D$. This sets a hard limit for how close in to the central star we can observe a planet. This doesn't pose a problem for the pinhole camera, since for most sun like stars the habitable zone is not expected to extend beyond 0.7 to 1.5 AU (Kasting et al. 1993). The size of the habitable zone also sets the minimum possible size of the pinhole, as $4\lambda/D$ must fall inside the habitable zone. Fluxes for each planet are normalized to the Earth assuming similar albedo and half-phase. Gaussian detector responses are convolved with an actual solar system map viewed orthogonal to the ecliptic to yield the results shown below. Our programs are capable of simulating systems viewed at any angle, but for simple comparison between different designs we will consider the same 90 degree inclination. Noise is simulated using standard Poisson statistics, and detector noise is negligible since photon counting detectors will be used in either configuration.

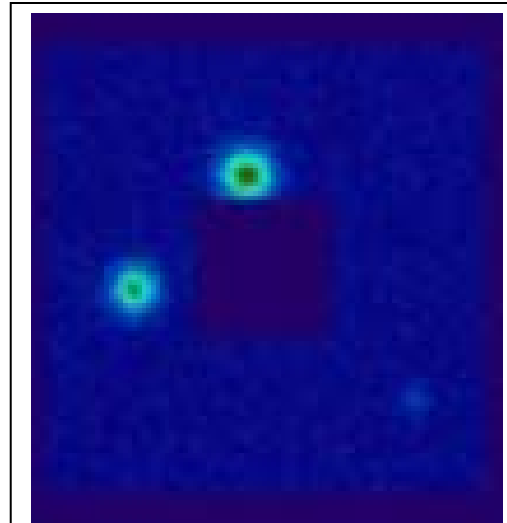


Figure 30: In a habitable zone survey it only takes a half day to detect Mars.

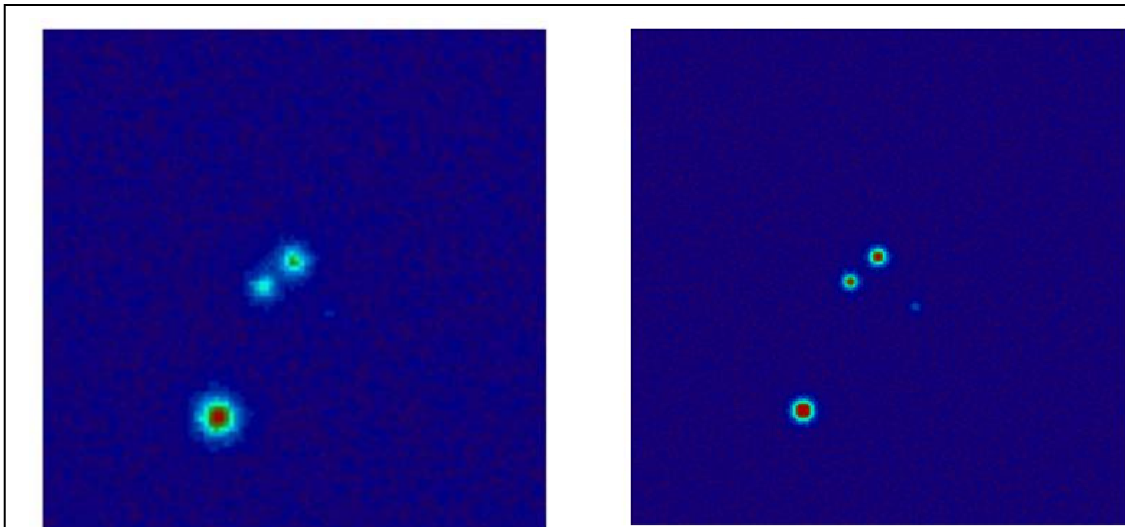


Figure 31: 50 ks integrations for the pinspeck configuration with a 1 meter and 4 meter telescope to the left and right, respectively.

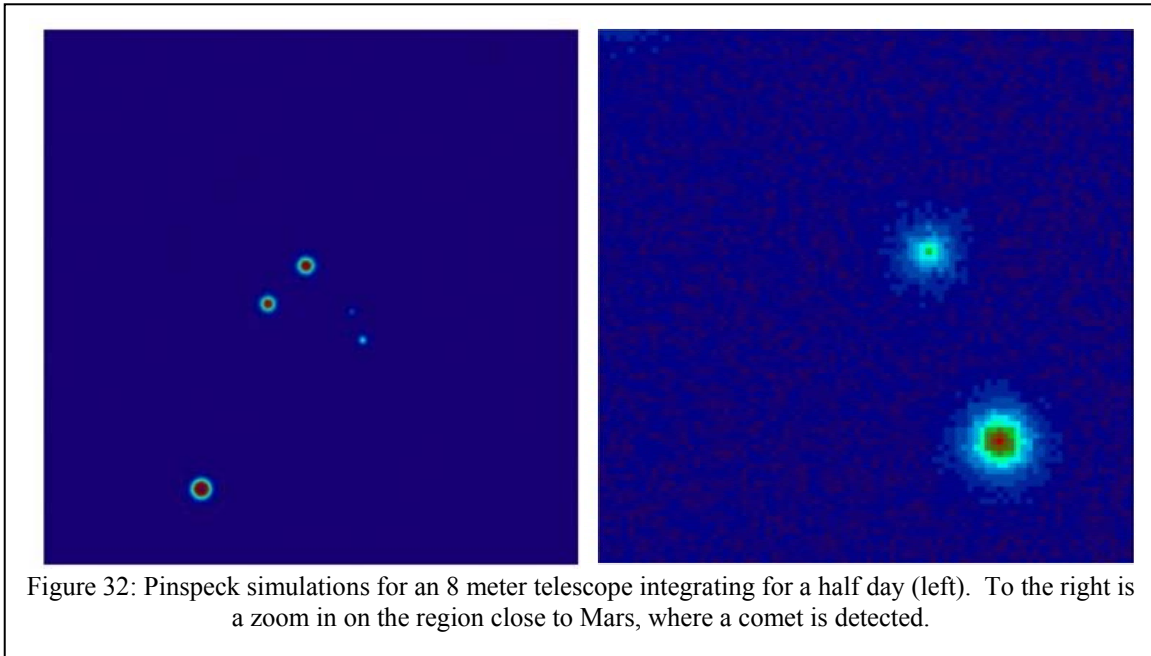
Simulations for 50 and 400 ks are shown in Figure 31. For the half day integrations Venus and Earth are easily detected and resolved, while a strong signal is detected from Jupiter. For this amount of coverage of the solar system, it requires two days to detect Mars. A habitable zone survey would only require a half day to detect Mars (Figure 30).

PINSPECK CAMERA : In the pinspeck configuration, a 10 to 20 meter shaped occulor diffracts the central starlight to create a hole in the middle of the focal plane with the needed 10^{10} contrast for planet detection. In this case the size of the hole is achieved by changing the occulor shape and size to achieve contrast over a large enough region to place a telescope. Since the Earth at 10 parsecs is separated from its star by 0.1", our telescope must be diffraction limited to 0.1" or better. This requires a 1 meter or larger diameter telescope and, correspondingly, a similar sized high contrast hole in which it may be placed.

Integrations were run for telescopes of 1, 2, 4, and 8 meter telescopes over periods of 50 to 400 ks. The pinspeck configuration is far superior to the pinhole camera for system mapping because the entire system is observed at once. Hence shorter integration times are required to achieve similar results. With a pinspeck the starlight is diffracted away from the center axis, so it is not necessary to block out the central region in our simulations. The simulated field of view is exactly the same as that in the previous simulations for easy comparison. Flux considerations are similar as well.

Figure 31 shows simulations for the one and four meter telescope with integration times of 50 ks. These show Mars can be detected in only a half day with a one meter telescope. Resolution is clearly improved with the 4 meter telescope, achieving 60,000 counts off the Earth over only ~ 4,000 counts with the one meter.

As long as the pinspeck is capable of creating a large enough high contrast region around the



central axis, it is possible to put a telescope of any size for detection. Larger telescope apertures allow for better resolution and quicker integration times. With only an 8 meter telescope it is possible to detect comets in only a half-day (Figure 32). This comet, at a distance of 1 AU is approximately as bright as Haley's comet would be under appropriate conditions. Smaller telescopes are of course capable of detecting similarly dim objects, however integration times are much longer and the resolution not as good.

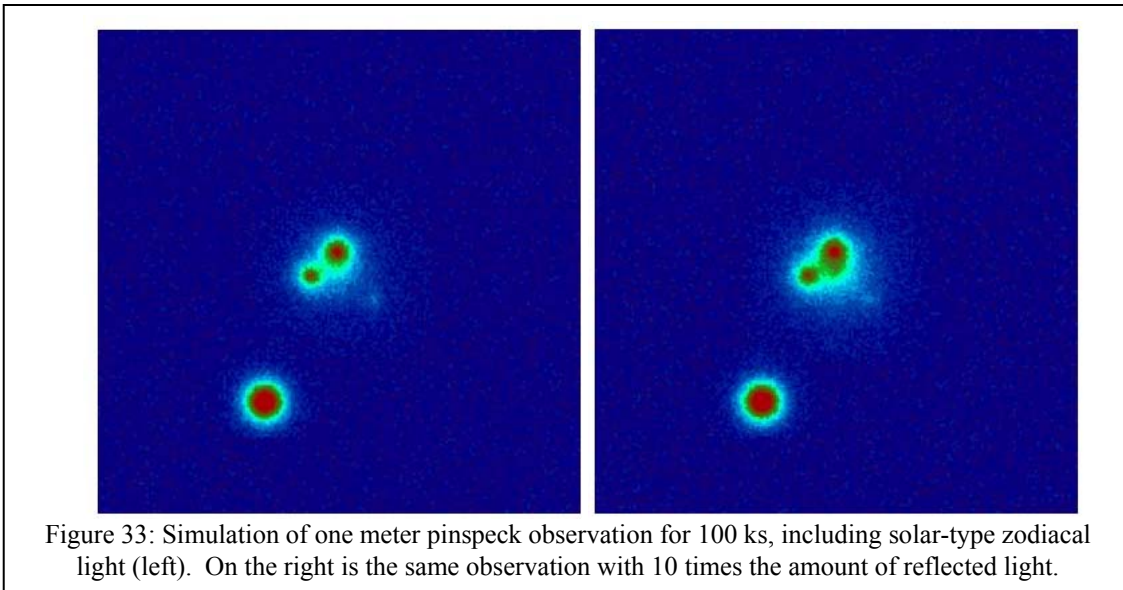
ZODIACAL LIGHT : As can be seen during any sunrise or sunset in a dark sky, starlight scattered off interplanetary dust particles creates a faint glow in the ecliptic plane of a solar system. This zodiacal light should be expected in other solar systems, and hence must be considered in simulating exoplanet detection. In the infrared, this background can hinder planet detection, since the emitted heat radiation from the dust particles could potentially overwhelm the

emitted thermal radiation of the planet. Fortunately NWO is not plagued by these problems, and the visible zodiacal light is not as strong.

For the purpose of our simulations we look to the zodiacal light distribution in our own solar system. Much research has been done through ground-based and satellite observations to quantify the amount of interplanetary dust in the inner solar system via its reflected starlight. Recent work by Hahn et al (2002) used the Clementine spacecraft to create a surface brightness map of visible zodiacal light during occultations of the sun by the moon. We use their fit to surface brightness vs. radius to map the zodiacal light in our observed solar system:

$$Z(r) = 1.7 \times 10^{-13} \left(\frac{\sqrt{1+r^2}}{r} \right)^{2.45} B_*$$

R is the radius from center of the solar system in AU, and B* is the solar brightness. The surface brightness of the zodiacal light drops off fairly quickly away from the sun. If we assume a similar amount of interplanetary dust around a solar type star we can expect similar behavior, and at 1 AU the zodiacal light is over one hundred times fainter than the Earth. This is seen in Figure 33, simulated along with a 1 meter aperture observation for 100 ks.

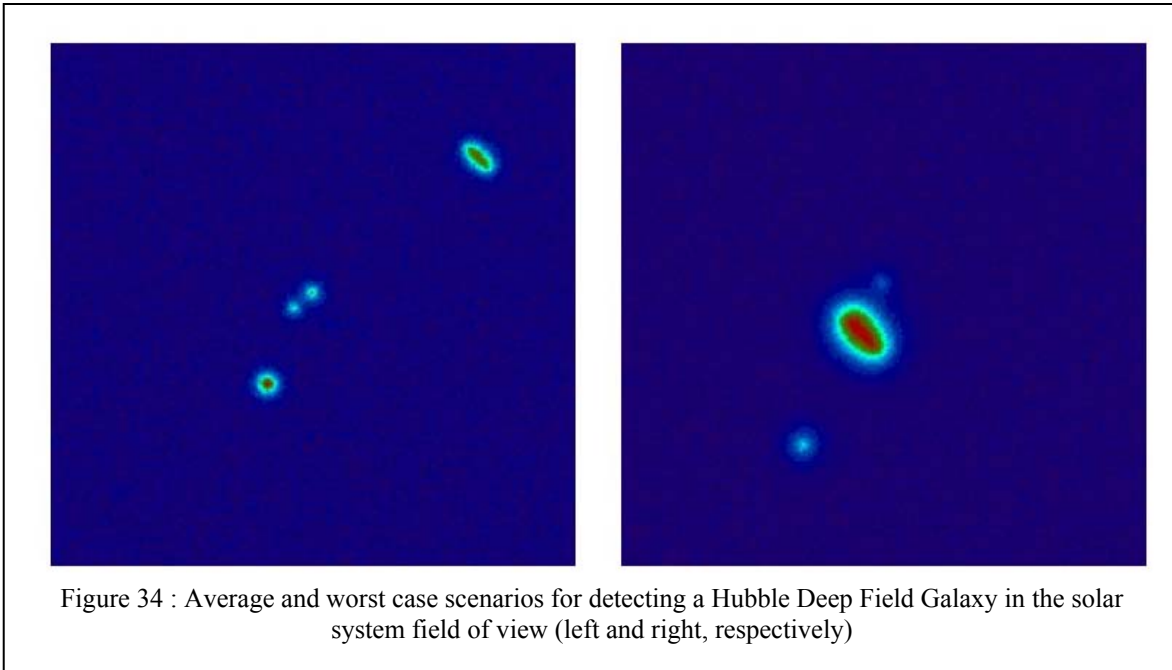


These simulations demonstrate that for any solar-type star with properties similar to our own solar system, zodiacal light should not pose a problem for planet detection in a face-on view. Even if there is enough interplanetary dust to increase the background by ten times, it should still be possible to detect terrestrial planets. Zodiacal light is only strong enough to be seen in the inner regions of the habitable zone, so it only really needs to be accounted for in the case of the pinspeck configuration. In the case of the pinhole camera, most of the zodiacal light would be contained in the inner $4\lambda/D$ which the moving telescope would not see.

DEEP FIELD GALAXIES: In 1995, the Hubble Space Telescope was pointed at a relatively dark spot in the northern latitudes of our galaxy for ten days to image the Hubble Deep Field (Williams et al. 1996). Covering one square arcminute, this exposure uncovered thousands of galaxies as deep as 30th magnitude. Approximately half of these are bright enough to be comparable to the Earth's radiance at 10 parsecs. In addition, some of the galaxies are large enough to cover a planet by a few times its size on the focal plane. In these studies we analyzed the feasibility of detecting planets with the presence of background deep field galaxies.

Using online catalogues of the detected deep field galaxies, we were able to compile statistics on the likelihood of misdetections. For our field of view studied above, there is an average likelihood of having one galaxy within 1 arcsecond of the central star. This is plotted in Figure 34, choosing an average luminosity as well. However, many of the Deep Field galaxies are extended, taking up several resolution elements of the telescope. The planets in our field are guaranteed to only fill one resolution element, so on average it will be very difficult to mistake a galaxy for a planet, and the galaxy will not be close enough to the star to overwhelm the planet's luminosity.

In the 90th percentile worst case scenario, the galaxy is not only extremely bright and extended, but it falls within the habitable zone of our observed system. In the unlikely chance



that this occurs, we would be certain we are seeing a galaxy. Dust disks or clouds around stars would not emit brightly in the visible, nor should they be so asymmetrical. Even if this does occur, the proper motion of the observed star would move it out of the way. The Hipparcos Space Astrometry mission has already catalogued the nearest several hundred stars which New Worlds would observe. All of these have proper motions on the order of 1 arcsecond per year (ESA 1997). Since multiple observations of star systems will be necessary to confirm and obtain planetary orbits, this will naturally alleviate any “temporary” galaxy detections.

The best case scenario is that the galaxy is too dim and too far away from the parent star to be detected in our surveys. There is of course the risk that one of these dim galaxies may fall in the field of view and be mistaken for a planet. The highest magnitude deep field galaxies would only be large enough to fill one resolution element, and are on the same order of brightness as Mars or a distant ice giant. However, this problem would be solved in the worst case scenario by enough observations to confirm motion of the galaxy in accordance with the proper motion of the star.

2. Planet Spectroscopy

The New Worlds Imager can provide high resolution spectroscopy from the far UV to the near IR with excellent sensitivity. New Worlds will be able to detect methane, water, oxygen, ozone, and other gases at Earth's current and past levels of concentration. NW will have high enough sensitivity and spectral resolution to detect important atmospheric signatures and chlorophyll-type absorption edges. By operating at visible wavelengths (which penetrate to the ground) NW will be able to determine the planet's rotation rate, presence of weather, and even the existence of

liquid oceans. Combined with atmospheric diagnostics, this information will extend the reach of biologists, geophysicists, and atmospheric chemists to worlds and ecosystems far beyond Earth.

Table 2: Spectroscopic Biomarkers

Water	Necessary for habitability
Oxygen	Free oxygen results only from active plant life
Ozone	Results from free oxygen
Nitrous Oxide	Another gas produced by living organisms
Methane	Life indicator if oxygen also present
Vegetation	Red edge of vegetation at 750nm

Most studies of Earth-like planet biosignatures to date have focused on present-day Earth or small variations of it. But experience in planetary exploration and exo-planet detection amply shows we should not be held hostage to our only example of planetary life. Indeed Earth has, in the past, exhibited different atmospheric signatures due to extreme climatic states such as glaciation, the rise of photosynthetic organisms, and methane bursts. Moreover, just as each of our rocky planets differs greatly from each other, there is no reason to expect extrasolar terrestrial planets to be similar to Earth. If a planetary atmosphere is determined to have a severe departure from chemical and thermodynamic equilibrium would we be able to identify the disequilibrium

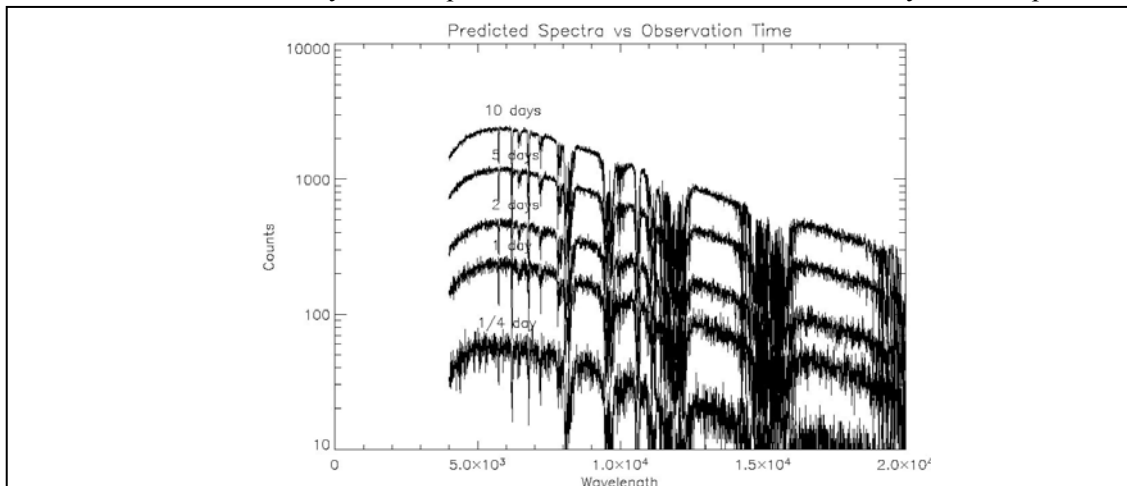


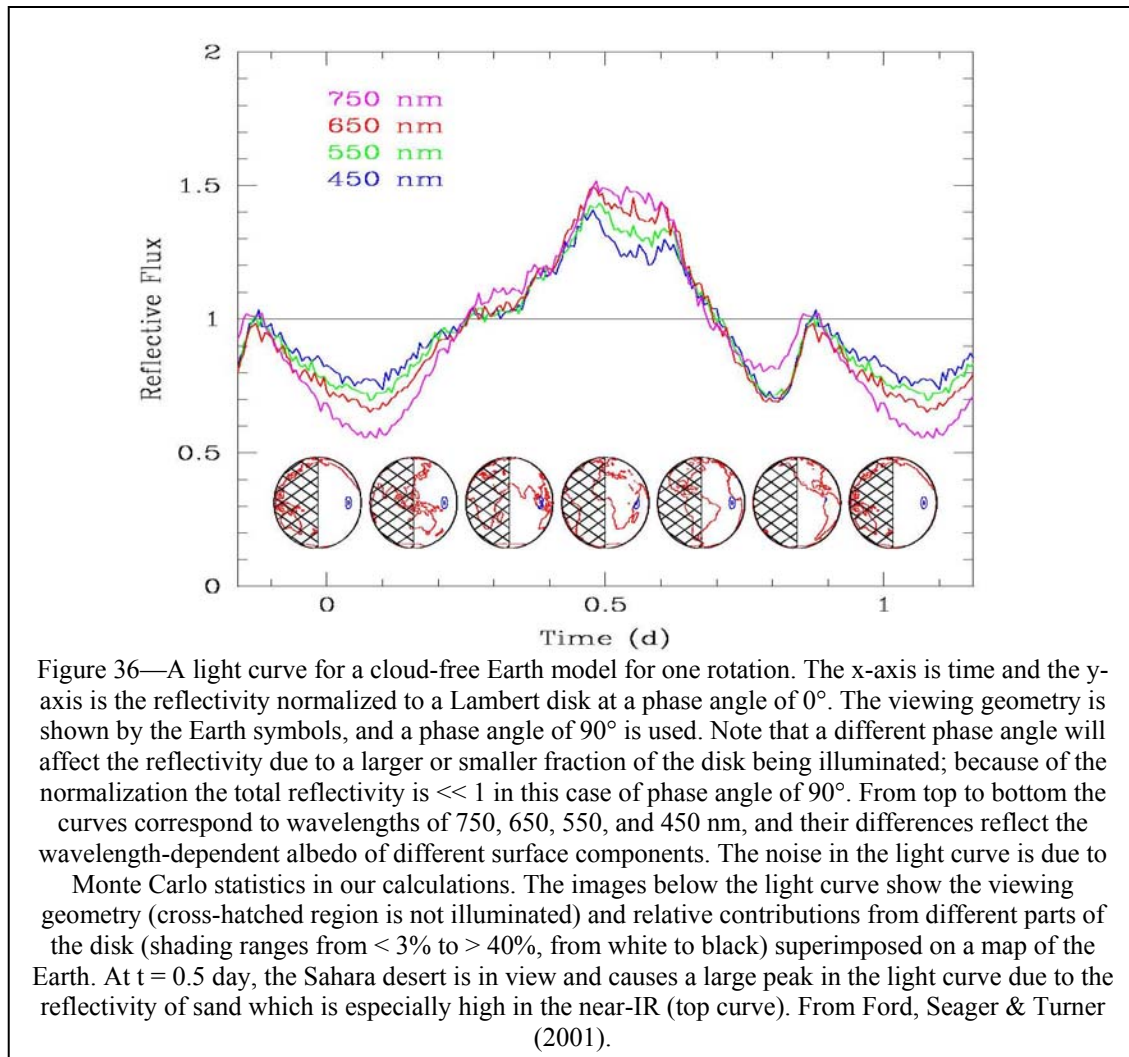
Figure 35: Simulated spectra of an Earth-like planet at 10pc taken with New Worlds. The data for this plot are by Co-I Seager.

features with biological modification of atmospheric composition? Or will there always be an ambiguity with geological processes? Will we be able to unambiguously identify a spectral signature not consistent with any known atomic, molecular, or mineral signature in the solar system and Universe (such as Earth's vegetation red edge)?

3. Photometry

PLANET IMAGING: For a suitably bright planet, a time series of sufficiently high quality spectro-photometric data could reveal a wealth of physical characteristics at wavelengths that penetrate to the planetary surface. Visible wavelengths are more suited for these measurements than mid-IR wavelengths because the albedo contrast of surface components is much greater than the temperature variation across the planet's surface. Moreover, the narrow transparent spectral window at 8-12 microns will close for warmer planets than Earth and for planets with more water vapor than Earth.

Earth is the most variable planet in our solar system, photometrically speaking. This variability is due to weather: cloud formation, motion, and dissipation. The variability at visible wavelengths is approximately 10 to 20% and is caused by the contrast in albedo between the reflective clouds and the underlying, darker land or ocean. Evidence of variable water clouds



combined with water vapor in the atmosphere is indicative of large bodies of liquid water. A variable planet would definitely warrant further study—compare the variable Earth to the constant, 100% cloud-covered Venus which shows relatively little change.

The rotation rate of a planet is an important physical characteristic because it is a fundamental driver of atmospheric circulation patterns and weather and it is a record of the planet's formation history. The rotation rate can be determined at visible wavelengths on a relatively cloud-free Earth-like planet if the planet has different surface components. The light scattered by such a planet will vary in intensity as the planet rotates, with a repetitive pattern. For example, Earth's major surface components (land, ocean, and ice) have very different albedos ($< 10\%$ for ocean, $> 30\text{-}40\%$ for land, $> 60\%$ for snow and some types of ice), and in the case of a cloud-free Earth viewed at the equator the rotational surface variation can be up to 200% (Figure 36). Even considering the Earth with its cloud patterns, the rotational period is still determinable because large-scale cloud formations persist coherently in some regions for several days.

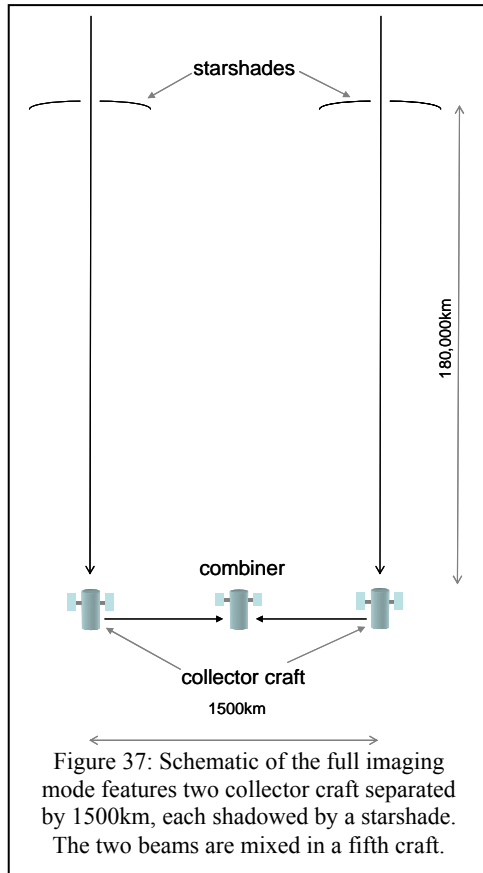
A terrestrial planet is likely to have a rotation period somewhere between an hour and a year. Since the interferometer will only detect on the order of 10 counts per second and the apertures

must travel many kilometers through the UV plane, it will take many hours to complete an exposure during which the planet will rotate. This means that to create a map of the surface, the first step is to establish the length of the planet's day through photometry. It is likely that the actual images will be built up through model-fitting to a rotating target. For a target like Mars, with no clouds, this will work well. There is some concern that moving cloud banks on a planet like Earth will change enough during the exposure that their motion will have to be independently modeled.

III. The New Worlds Imager

A. Concept

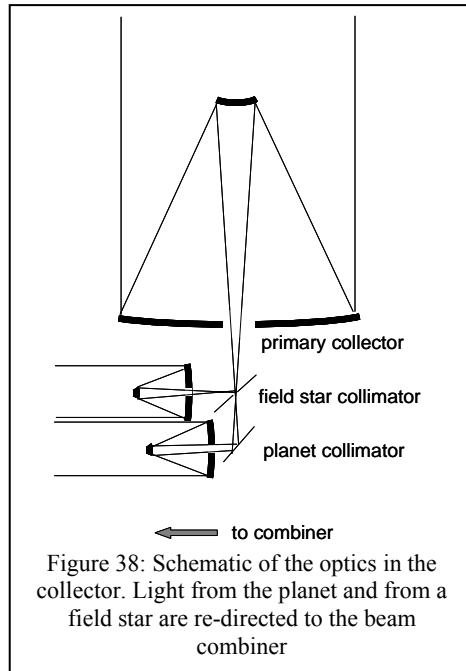
PLANET IMAGING: The overall architecture of the Planet Imager is presented in Figure 37. It involves five spacecraft flying in formation. Two starshades, two collector craft and one beam combiner craft.



The starshade and collector craft work just as for the observer mode, except that the beam is not detected in the collector. Figure 38 shows that the beam from the planet must pass through the craft where it is picked off and recollimated into a beam that is directed to the combiner craft. The entire array is monitored with a laser metrology net and the craft are held in position using microthrusters.

In the combiner craft two telescopes gather the light from the collector craft as shown in Figure 39. The two beams are then mixed to form fringes on a detector. The fringe visibility is measured at many points in the UV plane and then used to reconstruct an image in the manner of the radio astronomers.

For true planet imaging the goal would be to achieve 100km resolution in the visible at a distance of 10pc. That means a resolution of 3×10^{-13} radians, implying that the baseline of the interferometer must be about $3 \times 10^{12} \lambda$ or 1500km for yellow light. The diameter of a terrestrial planet is about 100 times that, so in order to fill in the UV plane,



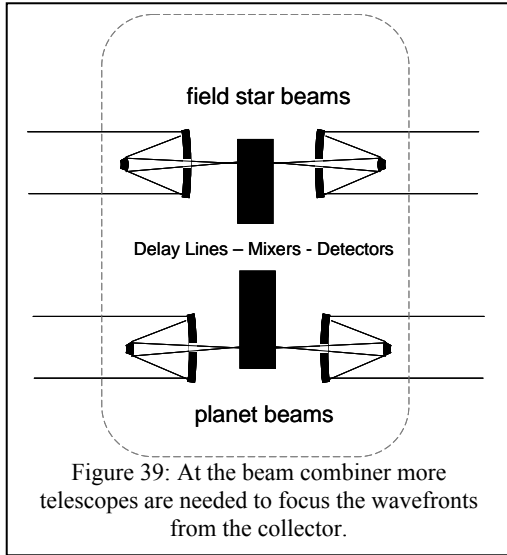
the interferometer also needs to operate at a distance as low as 15km. The beam combiner is on a separate craft half way between the two collectors in order that the total path from source to interferometer through the two apertures may be set equal.

The signal from the planet is passed through a collimator before it is sent to the beam combiner. To keep the beam from spreading significantly across the 1500km, the collimator must be a diffraction limited one meter aperture or larger – roughly 0.1 arcsecond quality.

At the combiner craft another telescope captures the (diffraction limited) wavefront from the collector craft and concentrates it. The two beams are mixed to create fringes. The fringe visibility is measured as a function of position in the UV plane and as a function of wavelength. The fringe visibilities are added in a manner similar to that performed in the radio to create the final image in a

computer. Design of the interferometer will be a subject of study, particularly in Phase II after the requirements are set.

Figure 38 and 39 also show optics for a “field star”. This is necessary for maintenance of pointing. Consider that 100km at 10pc represents 0.1micro-arcseconds resolution, so the slightest drift in pointing can ruin the image. The idea for maintenance of pointing is to use a field star, one that is outside the area occulted by the starshade but close enough to the center of the field of view of the collector scope that it remains diffraction (as opposed to aberration) limited. The light



from such a (presumably distant) star is picked off at the focal plane and sent through a separate collimator to the beam combiner craft. In the combiner craft there is a separate pair of telescopes that collect the star light and create fringes.

In practice it will be necessary to study the time scales and possible approaches to keeping the OPD small. For example, the beam combiner could contain a delay line similar to that in use on SIM (Space Interferometry Mission) that can compensate for smaller motions. On the other hand, small adjustments might be easier to make with micro-thrusters on the collector craft. Finding the zero OPD will be challenging. A number of approaches will be studied in the course of this effort.

B. The Interferometer

More detailed study of the interferometer and its requirements is needed. At its simplest, the two beams are focused to a spot where they cross at a low angle and create fringes across the Airy disk. However, at different wavelengths, the light beats at different frequencies, confusing surface feature effects with wavelength effects. The solution is to disperse the light in a small spectrometer, allowing clean fringes over a broad band. The resolution of this spectrometer is modest, about $\lambda/\delta\lambda=100$, the maximum number of resolution elements desired across the target.

C. Target Acquisition

The problem is not so much the drift in the distance from the combiner to the collectors, as that can be directly measured in the metrology net. The problem is the distance from the source (planet) to the collector. If the collector drifts toward the source or away, by even a micron, the fringes will shift in the combiner. The star, which is typically 20th magnitude is thousands of times brighter than the planet, and as a result will be able to rapidly detect a fraction of a wavelength shift in the total optical path difference.

D. Formation Flying

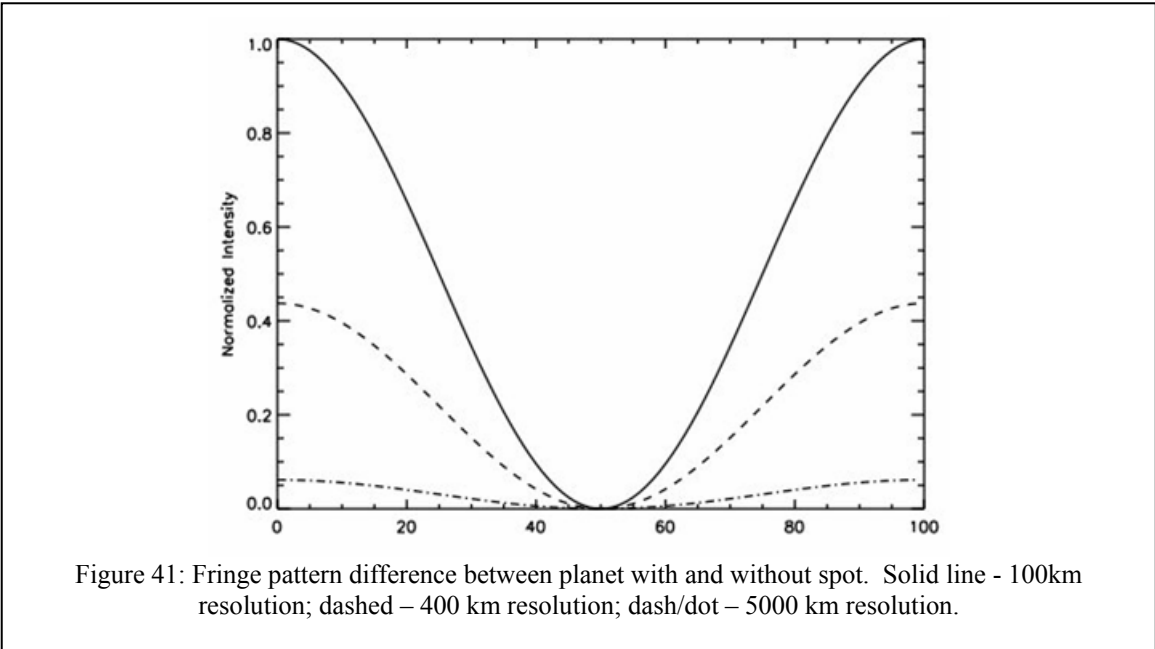
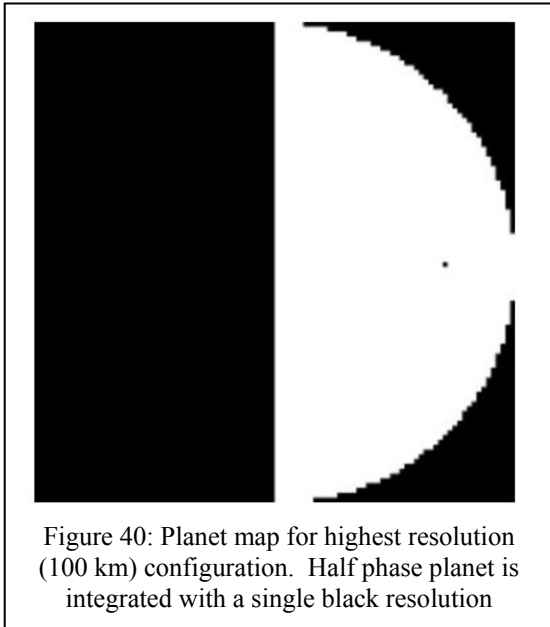
The formation flying for the interferometer will have to be somewhat better than for the New Worlds Observer. While the total path length must be nulled to a fraction of a micron, in practice the last few centimeters can be nulled in the combiner. Knowledge is

obtained from the metrology net and the stellar interferometer. Our calculations show that the perturbations at L2 will be sufficiently small that the drift rates can be detected and corrected.

E. Simulations

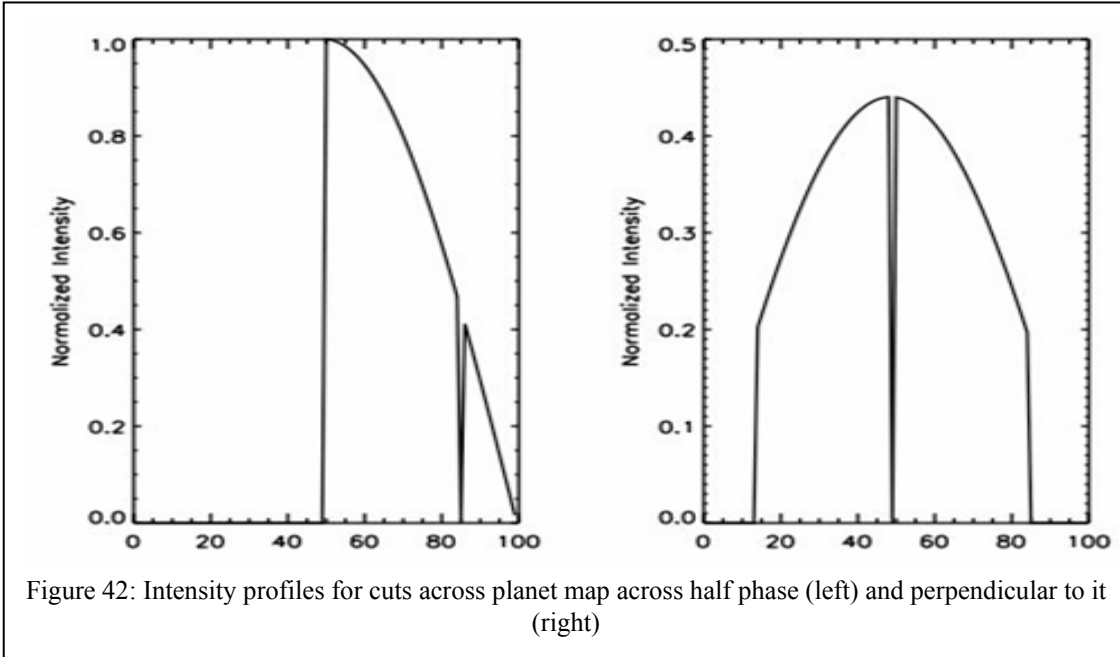
Using at least two Observers together as an interferometer, the New Worlds Imager will be able to resolve features on an extrasolar planet. As the spacecraft spiral through the UV plane, they will create fringes out of the combined planet light at different frequencies. These fringes will provide information about the intensity profile across the planet's surface at different resolutions. In order to understand necessary integration times for NWI, we simulate fringe patterns for simple variations in a planet's intensity profile. Our ability to detect these variations is limited by photon statistics for sufficiently filling in fringe patterns. Here we produce preliminary simulations to show we can detect the needed information in relatively short periods of time. Developing the actual image-formation algorithm will take longer.

For simplicity we approximate the incoming signal as sine waves of the same wavelength. These waves are assumed to be perfectly in phase from the diffracting pinspeck, so we can add them together depending upon where on the planet's surface they are coming from. The approximation of a singular wavelength will be loosened in



future simulations to assess optimum wavebands. For now, however, it is safe to choose one wavelength, as the resulting fringe patterns simply scale with wavelength.

At a given telescope separation B we sample photons from points across the planet's surface at a resolution of λ/B . A planet map is generated with the appropriate resolution, yielding the intensity for each wave. For the Earth at 10 parsecs, we simulate resolutions



of 100, 200, 400, 800, 1600, and 5000 kilometers. At each resolution, photons from adjacent bins are out of phase by $\lambda/2$ as defined by the interferometry. Sines are then added with intensity and phase according to position across the planet map.

For demonstration of concept a half phase planet is examined. For all additional simulations a half phase planet is used due to the average orbital configuration of the planet. A single resolution element is turned black, as shown in Figures 40 and 42. The resulting fringe patterns are analyzed for the planet face both with and without the

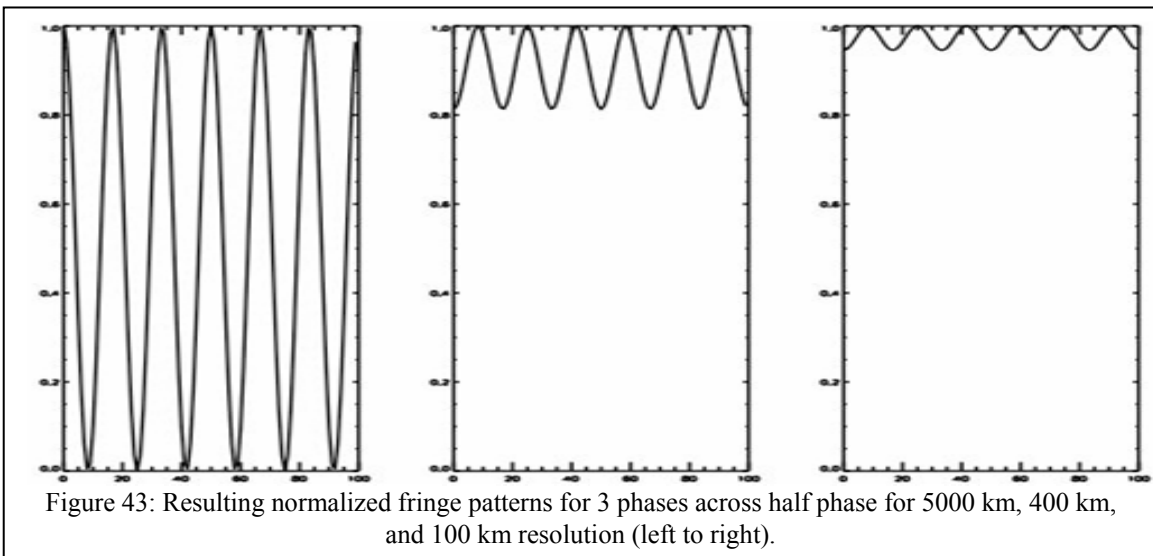
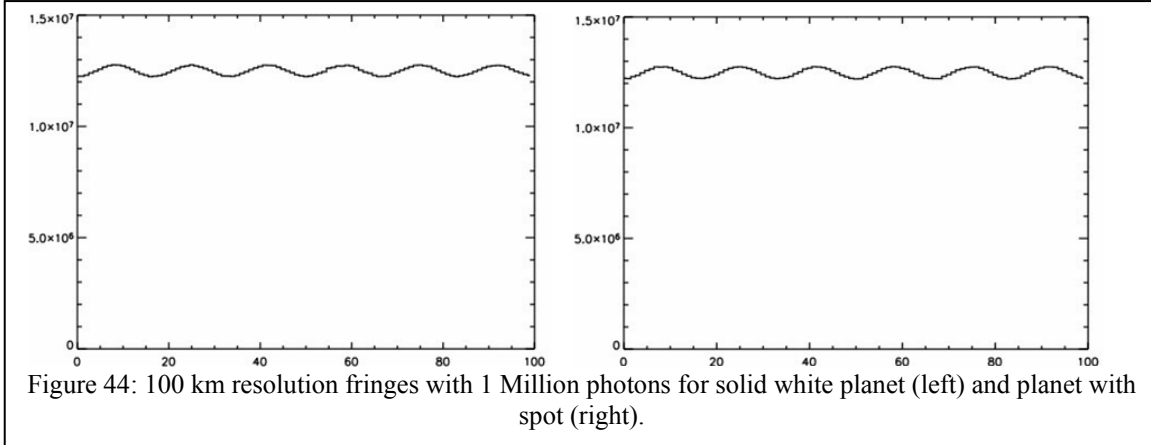


Figure 43: Resulting normalized fringe patterns for 3 phases across half phase for 5000 km, 400 km, and 100 km resolution (left to right).

spot. These fringes are generated from perpendicular paths intersecting at the spot of interest.

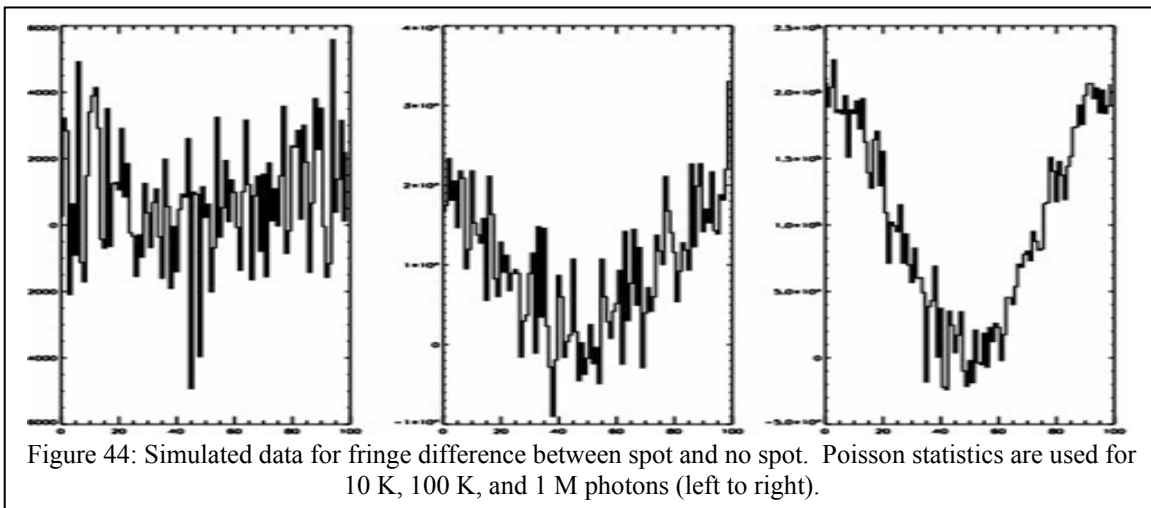
All the detectable information results from the one different pixel. Without the dark spot, the combined fringe pattern will add to a straight line, as all photons collected are of the same intensity. The difference in fringe patterns for the case of the spotless planet and the solid white planet is shown in Figure 41 at different resolutions. At the lowest resolution, the planet's two resolved points are only slightly different in intensity, and the



spot can barely be noticed. As the telescopes move further away and resolution increases, the spot becomes more apparent. At highest resolution the difference of a complete wave is seen.

In reality the planet's surface profile will vary greatly, and the fringes will not vary between a straight line and a sine wave. To approximate the change in intensity across the surface we use a profile which drops off towards the planet edge. Profiles intersecting at the black spot are shown in Figure 42. Realistically the center of the planet will contribute more information to the fringe patterns than the edges.

In this case the spot is harder to detect, as the change in intensity is not as great. However, information is still there as is shown in Figure 43. At the lowest resolution only two waves are seen, resulting in a pattern oscillating between 0 and 1. For higher resolutions a more complex pattern occurs, with variations between peaks harder to



detect. This information is what we will use in the end to determine features across the planet's surface.

Different separations around different azimuths will be combined to build up a complete image. The positioning of intensity variations across a single baseline path affects the phase of the collected photons. Only by convolving over the entire UV plane will it be possible to determine the positions of the detected features. The Observers will accomplish this by slowly spiraling out away from each other in the focal plane of the system.

Poisson statistics can be used to approximate how many photons are necessary to fill out a given fringe pattern. For proof of concept we simulate the fringe pattern caused by the presence of the spot for the profile in Figure 42, as well as that for the solid white planet. For 1 million photons, the resulting fringes are shown in Figure 44. They look nearly identical because the single black spot only subtly affects the wave pattern. Only one percent of the total photons are different between the two. It is this one percent difference we need to be able to detect if we are to perform the proposed imaging of the Earth at 10 parsecs.

It is thus more useful to look at the difference between the two patterns for a sign of the spot's presence. Shown in Figure 45, it is indeed possible to see the spot with enough photons. Clearly the difference is undetectable with only 10 thousand photons, but with 100 thousand photons structure is apparent. One million photons distinguish the spot's presence with certainty. Two 10 meter Observers could easily collect this much light in less than half a day.

IV. Preliminary Roadmap

A. Scaling the Architecture

It is always instructive to calculate just how far a technology can be taken before it hits limits. In this section we look at some of the limitations on the eventual performance of these systems.

1. Planet Finding

Planet finding at the moment is limited by the signal detected and the resolution of the telescope. With increased size (staying at the diffraction limit) both can be improved significantly. With 100m class optics and very long observations, it should be possible to detect objects many millions of times fainter than the Earth. Asteroids will become visible, and detailed dynamics of systems can be mapped.

2. Photometry

With a large increase in sensitivity and watching a planet through many rotations, it should be possible to sense very small features on the surface of planets. In essence, weather can be observed. But the interferometric imaging should make improvements in the photometry less important.

3. Astrometry

Astrometry can be improved by using the long baseline interferometry. Across a million or more kilometers the precision of the astrometry could reach 100 meters at 10pc. The uses of such precision are unclear at this time.

4. Spectroscopy

With increases in collecting area, it will be possible to create spectra of ever-higher quality. It is likely that spectra with resolution of up to 100,000 ($\lambda/\delta\lambda$) would be of value for scientific diagnostics of planets. This can be achieved with apertures not much larger than 10 meters. Beyond that point, there is little scientific reason for better spectra.

5. Imaging

We all want to see the pictures of planets around stars. The first attempt at imaging will be through watching the photometric variations of the planet as it rotates. Even a minimal New Worlds Observer would support these kinds of studies. To obtain true images of planets with resolutions as fine as 100km can be accomplished with 10m class telescopes at a separation of 1500km. This is an expensive mission but within the envelope of what NASA can afford. With long observations it may even be possible to perform point-by-point spectroscopy of the surface (with 100km resolution) to perform preliminary geological studies. But to truly study the surfaces in detail, the way missions like LandSat have of the Earth would take very large apertures, on the order of a square kilometer. This is unlikely to become affordable in the foreseeable future.

6. Surveys

A survey mission would be one that maps a thousand or more nearby planetary systems and then revisits each to map the orbits. With a requirement of up to five systems per day, this would require the delay between targets to be no more than about an hour. If we are to use multiple starshades, propelled by solar powered ion thrusters, it would take a fleet of dozens, possibly even one hundred. Perhaps this is not impossible if economies of scale kick in. After all, the starshade is a very simple craft. Alternatively, the starshade could be outfitted with a large booster, so it could travel from point to point at high speed. It is not clear which is more cost-effective. One thing is clear, however: if water planets turn out to be rare, then we may have to survey large numbers of stars to find that elusive blue dot.

7. Distance

The starshade has the function of creating a high contrast zone. But the distance between the starshade and the telescope rises as the square of the resolution. Since we can observe Earth-like planets at 10pc using a starshade at distances as small as 30,000km. To observe Earth-like planets at 100pc would require a starshade/telescope separation of 3million kilometers. While this is still possible it represents a practical upper limit.

8. Sensitivity

The starshades are capable of reducing background light to essentially zero. Similarly, low noise detectors are improving all the time. Thus sensitivity will be limited purely by signal and that will be a function of the collecting area. The collecting area can be increased either by increasing the size of the mirrors, or by increasing their number. In either case it would appear that we will be limited by cost.

B. Key Technologies

Most of the technology needed for New Worlds already exists and needs only be adapted. But, as is always the case, some technologies are more challenging than others. In this section we list those technologies and discuss what needs to be done.

1. Diffraction Controlled Apertures

The very existence of apertures that can create high contrast at low angular separation is what enables the New Worlds concept. Work is needed to understand these apertures at a flight level.

a) Optimization

We have just recently discovered a class of solutions to the pinspeck problem that is highly compelling. We are actively searching for optimal solutions, those that minimize costs and maximize performance. We expect to significantly decrease the projected cost over the next few months.

It is also quite possible that other classes of solution exist that may improve the system even more. We will continue to search for them. Since performance is already good, it is likely that an improvement would take the form of a smaller or easier-to-build starshade.

b) Tolerancing

It is a wonderful feature of the starshades that the sensitivity to error scales as the square root of the needed contrast rather than linearly. That is, to achieve 10^{-10} contrast requires that the shape have errors amounting to no more than 10^{-5} of the area. In a 100m shade this means that accumulated errors can amount to as much as a square foot before becoming a problem. But that statement alone, while giving us confidence that the starshade can be built to specification, does not translate directly into fabrication specifications. Extensive tolerancing will need to be performed, working closely with the starshade design and deployment scheme.

c) Laboratory Demonstration

Another attractive feature of the starshade is that it is based on the Fresnel integral only. Nobody questions the accuracy or appropriateness of the calculations. So, on the whole, there is confidence that the starshades will work the first time.

But it is equally true that one always learns important lessons about implementing a system when one builds and tests a prototype. The scaling of the starshades shows that separation of the two components scales as the square of the angular resolution. So, to achieve resolution of 0.1" one needs tens of thousands of kilometers. However, if one needs an arcminute of resolution, then the separation falls to tens of meters. A laboratory demonstration of high contrast from a shaped aperture would be very valuable.

2. Large Structures

The starshade will be large. Further study of the approaches to these thin, large structures is required to optimize costs.

a) Launch

Even if one is using 5mil plastic, the mass of a 150m diameter sheet becomes tons. The launch mass becomes the limiting factor. We hope the diffraction optimization will bring the mass down and allow the use of a smaller rocket. However, we are in a reasonable range. Rockets exist today that can do the job.

b) Deployment

Approaches to deployment will need continuing study. Any approach that reduces risk, mass, or cost should be studied, since this remains one of the areas where this mission differs from more conventional missions.

3. Formation Flying

Another technology driver critical to New Worlds, yet relatively new, is the formation flying. Two spacecraft must align to a distant star to better than a tenth of an arcsecond, and then hold that formation for an indefinite period.

a) Alignment Sensing

The first challenge is alignment sensing. At distances as high as 200,000km, the two craft will need telescopes to see each other. Radar might be used to reach a rough alignment. Then beacons on each craft will be used to find the other against the backdrop of the stars. The telescope craft will see the starshade and maneuver it toward the target star. Small changes in position, on the order of meters, will then move the starshade to the full null position. At that point, the position of the telescope craft in the field of view of the starshade's telescope will be recorded, and the craft will maneuver to keep it fixed. There are many details that need to be worked out.

b) Microthrusters

In Phase I we showed that the orbital forces at L2 that pull the craft apart can be offset using ion micro-thrusters. Powered by solar panels, these thrusters can run continuously for years without running out of fuel and are ideal for our application. More details of these thrusters need to be incorporated into the plan.

c) Retargeting

One drawback of the New Worlds approach is the large distance that one of the craft must travel when a new target is to be acquired. We need to study approaches to this problem. For example, the telescope could simply be used for other science during travel times. We could build two starshades, with one traveling while the other observes. A third approach is to mount some larger thrusters on the starshade to give it extra speed.

d) Orbit

Preliminary studies by Northrop-Grumman show that L2 is an excellent environment for the New Worlds. However, the stationing and station-keeping of two craft in alignment still needs to be studied in detail.

4. Telescope

We have been relying on existing knowledge of telescopes from members of the New Worlds team (e.g. J. Green who is PI on the MUST vision mission study). More study of the telescope and their requirements is needed.

C. The Road Ahead

Of one thing we are sure: The New Worlds concept will happen in two stages. There is no chance that a full, New Worlds Imager will be implemented until the efficacy of starshades has been proven in a New Worlds Observer class mission. Simultaneously, the scientific return of the NWO is so high that it makes sense as a stand-alone mission. Indeed, without a preceding planet finding mission like NWO, an imaging mission would not know where to look.

We believe that the New Worlds Observer can be implemented now and that it is timely to do so. We may be able to provide the much-desired results faster and cheaper than can be done with TPF. Finishing the study to the point where all questions are answered and all technologies are at a high level of technological readiness (i.e. ~TRL 6) is a high priority.

There are three ways to implement the New Worlds Observer. The first is to build and fly a pair of dedicated spacecraft. The second is to build and fly only a starshade, but to use an existing space telescope (e.g. JWST) to observe. The third possibility (cheaper and less effective) is to place the observatory on the ground, most likely at the South Pole, where its motion is small. Then we fly the starshade above the observatory to create a null zone through the scattering of the atmosphere.

We plan to approach NASA for support as soon as we have solid answers for the remaining questions. However, if sufficiently inexpensive versions of the NWO emerge, then the mission has all the right characteristics to allow alternative funding, such as from private donors.

As we complete our detailed studies of the NWO we will perform a full design analysis of the New Worlds Imager. Details of how to build a cost-effective interferometer will take center stage. Ironically, for the imager, the starshades will be a relatively simple and well-understood component.

V. BIBLIOGRAPHY

1. D. J. Des Marais, M. Harwit, K. Jucks, J. Kasting, D. Lin, J. Lunine, J. Schneider, S. Seager, W. Traub and N. Woolf, Remote Sensing of Planetary Properties and Biosignatures on Extrasolar Terrestrial Planets, *Astrobiology*, 2, 153 (2002)
2. N.J. Woolf, P.S. Smith, W.A. Traub, K.W. Jucks, The Spectrum of Earthshine: A Pale Blue Dot Observed from the Ground, *ApJ* (2002) 574, 430
3. L. Arnold, S. Gillet, O. Lardière, P. Riaud, J. Schneider, A test for the search for life on extrasolar planets: Looking for the terrestrial vegetation signature in the Earthshine spectrum, *A&A*, 392, 231 (2002).
4. ESA, The Hipparcos and Tycho Catalogues, ESA SP-1200, 1997
5. E.B. Ford, S. Seager, E.L. Turner, Characterization of Extrasolar Terrestrial Planets from Diurnal Photometric Variability, *Nature* 412 (2001) 885-887
6. Seager, S., Whitney, B. A., and Sasselov, D. D., *ApJ*, **540**, pp. 504-520. (2000).
7. Arking and Potter 1966, *AJ* 71, 154
8. Hahn J.M., Zook H.A., Cooper B., & Sunkara B., Clementine Observations of the Zodiacal Light and the Dust Content of the Inner Solar System, *Icarus*, 158, pp.360-378, 2002.
9. Hansen, J. E. and Hovenier, J. W. Proceedings of the Symposium, Torun, Poland, September 5-8, 1973. (A75-21276 08-91) Dordrecht, D. Reidel Publishing Co., 1974, p. 197-200. (1974)
10. Hecht, Eugene. "Optics" ©1998 Addison Wesley Longman Inc.
11. Kasting J., Whitmire D., Reynolds R., Habitable Zones around Main Sequence Stars, *Icarus*, 101, pp. 108-128, 1993.
12. F. Selsis, D. Despois, J.-P. Parisot, Signature of life on exoplanets: can Darwin produce false positive detections?, *A&A*, 2002, 388, 985
13. Pilcher, C. *Astrobiology*, in press (2003)
14. Copi, C. J., and Starkman, G. D., *ApJ*, **532**, 581-592, 2000
15. D. N. Spergel, "A new pupil for detecting extrasolar planets", astro-ph/0101142, 2000
16. Simmons, Bill. An Optimal Pinspeck Camera for Exo-Planet Spectroscopy Masters Thesis, Princeton, June 2005
17. D. Slepian. Analytic solution of two apodization problems. *Journal of the Optical Society of America*, 55(9):1110P1115, 1965.
18. N.J. Kasdin, R.J. Vanderbei, D.N. Spergel, and M.G. Littman. Extrasolar Planet Finding via Optimal Apodized and Shaped Pupil Coronagraphs. *Astrophysical Journal*, 582:1147P1161, 2003.

19. Williams et al., The Hubble Deep Field: Observations, Data Reduction, and Galaxy Photometry, *AJ*, 112, p.1335, 1996.
20. R.J. Vanderbei. LOQO userXs manualCversion 3.10. Optimization Methods and Software, 12: 485P514, 1999.
21. R.J. Vanderbei. Linear Programming: Foundations and Extensions. Kluwer Academic Publishers, 2nd edition, 2001.
22. R.J. Vanderbei, D.N. Spergel, and N.J. Kasdin. Circularly Symmetric Apodization via Star-shaped Masks. *Astrophysical Journal*, **599**, 686-694 (2003).